



Hiroshima University
Graduate School of Engineering
Department of System Cybernetics

Optimal Voltage Control for Active Distribution Systems Using Multi-Agents

(マルチエージェントを用いた配電システムの最適電圧制御)

PhD Dissertation

by

Ahmed Bedawy Khalifa Hussien

March 2020

Optimal Voltage Control for Active Distribution Systems Using Multi-Agents

(マルチエージェントを用いた配電システムの最適電圧制御)

by

Ahmed Bedawy Khalifa Hussien

D174893

A Thesis

Submitted to the Graduate School of Engineering
Hiroshima University

in partial fulfillment of the requirements for the Degree of Doctor of
Philosophy



Hiroshima University, Japan

March 2020

Abstract

The rapid increase in the installation of distributed generations (DGs), particularly solar photovoltaic (PV) associated with unbalanced features of distribution systems (DS), disturbs the classic control strategy of voltage regulation devices. The classic control strategies of the traditional voltage regulation devices, such as the on-load tap changer (OLTC), switchable capacitors (SC) and step voltage regulators (SVRs), are designed based on the unidirectionally power flow scheme from the substation to the loads. The DG installation changes the characteristic of the DS from passive to active, which can mislead such classic control strategies and causes tap oscillations and increase the voltage violation problems, i.e., voltage rise, voltage fluctuation and voltage imbalance because of the intermittent and unbalanced outputs of DGs.

The main objective of this work is to develop effective voltage control schemes for DS with high DG penetration. For this purpose, three strategies for voltage control are proposed in this work based on a multi-agent system (MAS) architecture. An advantageous feature of using the MAS scheme is a robust control performance in a flexible and reliable manner, even in the case of agent failure.

Firstly, an effective voltage control strategy for voltage regulators in the unbalanced DS (UDS) is proposed based on voltage/tap sensitivity and the MAS architecture. The features of the UDS with DGs and different types and configurations of voltage regulators are considered in the proposed strategy. The novelty of the proposed method lies in realizing both the control optimality of minimizing voltage violations and the flexibility to accommodate changes in the DS topology using a MAS scheme. Simulation studies have been conducted using the IEEE 34-node and 123-node distribution test feeders considering high PV penetration and different sun profiles. The results show that the proposed voltage control strategy can optimally and effectively manage the voltage regulators in the UDS, which decreases their operation stresses and minimize the overall voltage deviation.

Secondly, a simple and efficient method is proposed for voltage regulation by managing the reactive power of the DG sources. The proposed control strategy is formulated based on voltage/reactive power sensitivity analysis using the MAS architecture. Comprehensive case studies on IEEE 33 test feeders are carried out to demonstrate the effectiveness of the control strategy. The numerical results show that the

proposed strategy can significantly mitigate voltage violation problems in a simple manner.

Finally, a novel method for management the output active and reactive powers of the DG sources in order to realize an optimal operation of the DS. The objective of the proposed method is to control the reactive power outputs of DGs for maximizing the total output power while improving the voltage profiles of the DS. The proposed method resolves all those problems. In order to mitigate the voltage violation, the proposed method performs an optimal power flow (OPF) calculation and compute the nodal prices of active and reactive powers based on the MAS approach. Then dynamic pricing is carried out on-line using locational marginal pricing (LMP) for real and reactive powers of PVs in DS. The simulation results confirm that the proposed method can successfully deal with the voltage violations in DS and minimize the curtailment of PV power.

Acknowledgement

First and foremost, praises and thanks to Allah, the Almighty, for his abundance of grace, kindness, and blessings which gave me the strength to complete this research successfully. I would like to take this opportunity to express my deep and sincere gratitude to all those who helped me directly or indirectly for completing this research work.

I would like to thank all my colleagues working at the Electrical Power and Energy System Laboratory (EPESL), Graduate School of Engineering, Hiroshima University, for giving me the opportunity to complete this thesis and the friendly atmosphere that is indispensable to me. Especially, I would like to express my gratitude to my advisor Prof. Naoto Yorino for his professional support during my study in Japan. His valuable suggestions, guidance, and continuous support in every aspect to accomplish my PhD study. Also, I would like to express my gratitude to my sub-advisors Prof. Katsuhiko Takahashi and Prof. Ichirou Nishizaki.

I would like to express my greatest gratitude to all staff members of EPESL laboratory, especially Prof. Yoshifumi Zoka and Prof. Yutaka Sasaki who aided me at all research steps as well as living in Japan.

Also, I would like to thank the Egyptian Ministry of Higher Education for their fund of my study in Japan. Also, I would like to thank my Egyptian colleague Dr. Karar Mahmoud for the motivation and the continuous support of my PhD study and research.

Last but not least, I am grateful to all my family members: my parents, my wife, my children, and my friends for supporting me spiritually throughout my life. This thesis would not have been possible without their constant love and support.

Ahmed Bedawy

2020

Table of Contents

Abstract	I
Acknowledgement	III
Table of Contents	IV
List of Figures	VII
List of Tables	IX
Abbreviations	X
Chapter 1: Introduction	11
1.1 Research Background.....	11
1.2 Research Objectives.....	13
1.2.1 Management of Voltage Regulators.....	13
1.2.2 Management of DGs Power.....	14
1.2.2.1 Reactive Power Control of DGs.....	14
1.2.2.2 Active/Reactive Power Control of DGs Using Nodal Prices.....	14
1.3 Thesis Outline.....	15
Chapter 2: Voltage Control in Distribution Systems	17
2.1 Introduction.....	17
2.2 Distribution System Characteristics.....	17
2.3 Impact of DGs on Feeder Voltage Regulation.....	17
2.4 Voltage Control Techniques.....	19
2.4.1 Tap Changing Transformers.....	19
2.4.2 Shunt Capacitors (SC).....	20
2.4.3 Static Synchronous Compensator (STATCOM).....	20
2.4.4 Energy Storage Systems (ESS).....	20
2.4.5 Network Reconfiguration.....	21
2.4.6 Active/Reactive Power Control of the DGs.....	21
2.4.7 Cooperative Control Techniques.....	22
2.5 Control Structures.....	22
2.6 Multi-Agent System (MAS).....	23
2.6.1 MAS Architectures.....	23
2.6.2 MAS for Feeder Voltage Regulation.....	26
2.7 Summary.....	26
Chapter 3: Optimal Control Strategy for Voltage Regulators in Active UDS	27
3.1 Introduction.....	27
3.2 Proposed Control Strategy.....	27
3.2.1 Proposed MAS Control Strategy for the UDS.....	27
3.2.2 Optimal voltage control strategy.....	28
3.3 Control Method Formulation.....	29

3.3.1 Mathematical formulation	29
3.3.2 Proposed Control Rules.....	31
3.3.3 Formula of Index S	32
3.4 Formulation of Voltage/tap Sensitivity Matrix.....	33
3.4.1 Single-phase Regulators	33
3.4.2 Three-phase Star Connected Regulators	33
3.4.2.1 Three Taps Ganged Together	33
3.4.2.2 Three Independently Controlled Regulators.....	34
3.4.3 Three-Phase Delta Connected Regulators	34
3.4.3.1 Closed Delta	34
3.4.3.2 Open Delta.....	35
3.5 Control Procedure.....	35
3.5.1 Agent Measurement Process	35
3.5.2 Agent Calculation Process.....	35
3.5.3 Agent Data Collection	36
3.5.4 Agent Control Action:	37
3.6 Results and Discussion	37
3.6.1 IEEE 123-node Test Feeder	37
3.6.1.1 Case Studies	38
3.6.1.2 Overall Performance Evaluations	44
3.6.2 IEEE 34-node Test Feeder	45
3.7 Conclusions	46
Chapter 4: Reactive Power Control of the DGs for Voltage Regulation.....	47
4.1 Introduction	47
4.2 Problem Description.....	47
4.2.1 Objective Function	47
4.2.2 Control Strategy of Voltage Regulators	48
4.2.3 Voltage Control Problem.....	48
4.2.4 Time Coordination	48
4.3 Reactive Power Control Strategy	48
4.3.1 Control Strategy	48
4.3.2 Voltage/Reactive Power Sensitivity Matrix	49
4.3.3 Reactive Power Index (RPI).....	50
4.4 Control Process.....	51
4.4.1 Monitoring Process.....	51
4.4.2 Control Process of the Management Agent.....	52
4.4.3 Control Process of the Local Agents.....	52
4.5 Result and Discussion.....	53
4.5.1 Test Feeder	53

4.5.2 Simulated Cases	53
4.5.2.1 Case 1: Low PV Penetration	53
4.5.2.2 Case 2: High PV Penetration	55
4.6 Conclusions.....	56
Chapter 5: Active/Reactive Power Control of DGs Using Nodal Prices	57
5.1 Introduction.....	57
5.2 Proposed Control Strategy	57
5.2.1 Outline of the Proposed Strategy	57
5.2.2 Global OPF Formulation for the Management Agent	58
5.2.3 Formulation of KKT Condition for Global OPF	59
5.2.4 Profit Maximization for Local Agents.....	61
5.3 Control Process	62
5.3.1 Procedure for Management Agent.....	62
5.3.2 Procedure for Local Agent i	63
5.4 Simulation Results	63
5.4.1 Simulation Cases.....	63
5.4.1.1 Case1: Analysis of A specific Operating Point.....	64
5.4.1.2 Case2: 24-hour Simulation.....	65
5.4.2 Effect of Control Cycle on the Control Performance	68
5.5 Conclusions.....	68
Chapter 6: Conclusions and Future works.....	69
6.1 Novelty and Conclusions of the Dissertation.....	69
6.2 Future Works.....	70
References.....	71
Appendix A: Description of Test Systems.....	77
A.1 IEEE 34-node Test Feeder	77
A.2 IEEE 123-node Test Feeder	78
A.3 33-Bus Distribution System	78
A.4 5-bus Test Feeder	78
Appendix B: The Optimality of the Voltage Regulators Control Strategy.....	79
Appendix C: Conventional Method for PV Inverter Control.....	83
Appendix D: IEEE PES Japan Joint Chapter Best Paper Award	84
List of Publications	85

List of Figures

Figure 1.1 Annual additions of renewable power and total, 2012-2018 [1].	11
Figure 1.2 Traditional and active distribution system structures.	12
Figure 1.3 Structure of the thesis.	16
Figure 2.1 Voltage profile before and after addition of large DG.	18
Figure 2.2 Basic communication in the MAS [80].	24
Figure 2.3 Centralized MAS architecture.	25
Figure 2.4 Hierarchical MAS architecture.	25
Figure 3.1 Proposed MAS for the UDS.	28
Figure 3.2 Proposed voltage control method.	35
Figure 3.3 Utilized voltage control parameters in area k.	36
Figure 3.4 IEEE 123-node test feeder.	37
Figure 3.5 Total active and reactive power of the loads and PV.	38
Figure 3.6 Results of Case 0: Without control for the clear day.	39
Figure 3.7 Results of Case 0: Without control for the cloudy day.	40
Figure 3.8 Results of the proposed controls for the clear day. (Solid lines: case C1 (Optimal); Dashed lines: case C2 (Suboptimal)).	40
Figure 3.9 Results of the proposed controls for the cloudy day. (Solid lines: case C1 (Optimal); Dashed lines: case C2 (Suboptimal)).	41
Figure 3.10 Results of case 3: Proposed control for the cloudy day with failure.	42
Figure 3.11 Results of case 4: Conventional control for the clear day.	43
Figure 3.12 Results of case 4: Conventional control for the cloudy day.	43
Figure 3.13 Voltage deviation vs. tap change in clear day for different α and α_0 .	44
Figure 3.14 IEEE 34-node test feeder.	45
Figure 3.15 Voltage profile of node 890 (phase A).	45
Figure 4.1 Control strategy of DGs reactive power.	51
Figure 4.2 Flowchart of the control process.	51
Figure 4.3 IEEE 33-bus test feeder.	53
Figure 4.4 Load and PV curves.	53
Figure 4.5 Voltage profiles of Case1(Low PV Penetration).	54
Figure 4.6 Reactive power output of PV sources(Low PV Penetration).	54
Figure 4.7 Voltage profiles of Case 2(High PV Penetration).	55
Figure 4.8 Reactive power output of PV sources (High PV penetration).	55
Figure 5.1 Proposed Control System.	58
Figure 5.2 The control process of the proposed method.	62
Figure 5.3 5-bus test feeder.	63
Figure 5.4 Real load and PV output pattern for simulation.	65

Figure 5.5 Voltage profiles.	66
Figure 5.6 Conventional method vs. proposed method.....	67
Figure 5.7 Total voltage violations vs. control cycle for 24-hours (RMS p.u).	68
Figure A.1 IEEE 34-node test feeder.....	77
Figure A.2 IEEE 123-node test feeder.....	77
Figure A.3 33-bus test feeder.....	78
Figure A.4 5-bus test feeder.....	78
Figure C.1 Inverter control scheme for conventional method.	83

List of Tables

Table 3.1 IEEE 123-node test feeder regulator data.....	38
Table 3.2 Total voltage deviation and no. of tap changes	43
Table 3.3 Results of the IEEE 34-node test feeder.....	45
Table 5.1 Comparison of the conventional and the proposed method (Case 1).....	64
Table 5.2 Prices of P and Q offered by the management agent	64
Table 5.3 Generated powers and profits for 24-hour simulation (Case 2)	65

Abbreviations

APC	Active Power Curtailment
BESS	Battery Energy Storage Systems
BM	Blackboard Memory
DG	Distributed Generation
DS	Distribution System
ESS	Energy Storage Systems
IEEE	Institute of Electrical Electronic Engineering
KKT	Karush-Kuhn-Tucker
LDC	Line Drop Compensation
LMP	Locational Marginal Pricing
MAS	Multi-Agent System
MV	Medium Voltage
OLTC	On-Load Tap Changer
OPF	Optimal Power Flow
p.u.	Per Unit
PV	Photovoltaic
RES	Renewable Energy Sources
RPI	Reactive Power Index
SVR	Step Voltage Regulator
STATCOM	Static Synchronous Compensator
UDS	Unbalanced Distribution System
WTGS	Wind Turbine Generation System

Chapter 1: Introduction

1.1 Research Background

Recently, the installation of distributed generations (DGs) in distribution systems (DS) has quickly expanded; approximately 181 gigawatts (GW) of renewable power energy has been installed in 2018 worldwide, and 55% of this capacity is generated from solar photovoltaic (PV) sources as shown in Figure 1.1 [1]. This increase causes serious voltage problems in the DS. The DGs installation changes the characteristic of a DS from passive to active, which causes voltage rise, voltage fluctuation and voltage imbalance because of the intermittent and the unbalanced of the DGs outputs [2]–[5]. Figure 1.2 illustrates the structures of traditional and active DS (i.e., without and with DG integration).

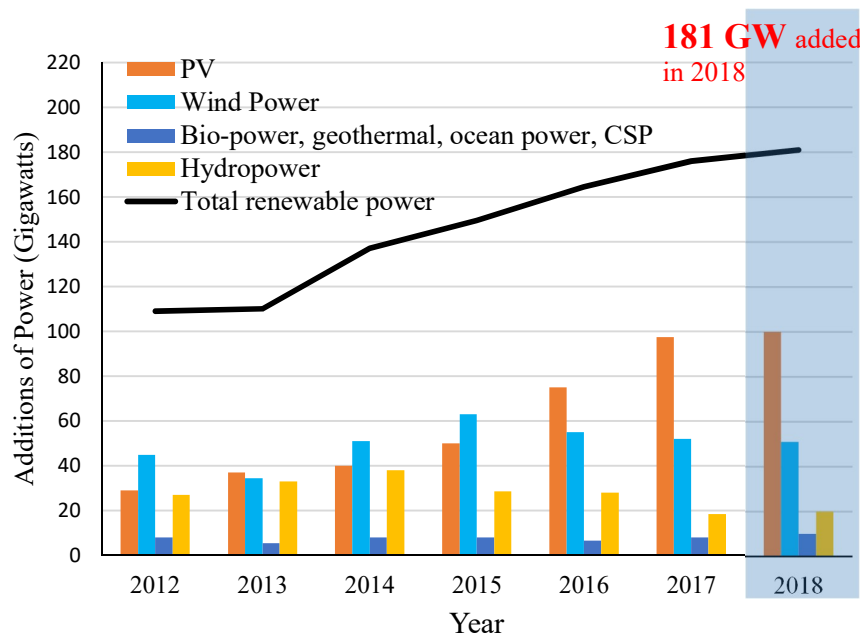


Figure 1.1 Annual additions of renewable power and total, 2012-2018 [1].

The classic control strategies of the traditional voltage regulation devices, such as the on-load tap changer (OLTC), switchable capacitors (SC) and step voltage regulators (SVRs), are designed based on the unidirectional power flow scheme from the substation to the loads. The bidirectional power flow caused by the DGs generation can mislead such classic control strategies and cause voltage violations and tap oscillations of the transformers. Various studies for voltage control have been performed, such as the local coordination techniques [6], [7], optimization techniques [8]–[10], neural network

applications [11], [12], and agent-based techniques [13]–[17]. Various strategies have been conducted to mitigate the impact of the high DG penetration on the DS voltage. The approaches can be classified into centralized and distributed methods.

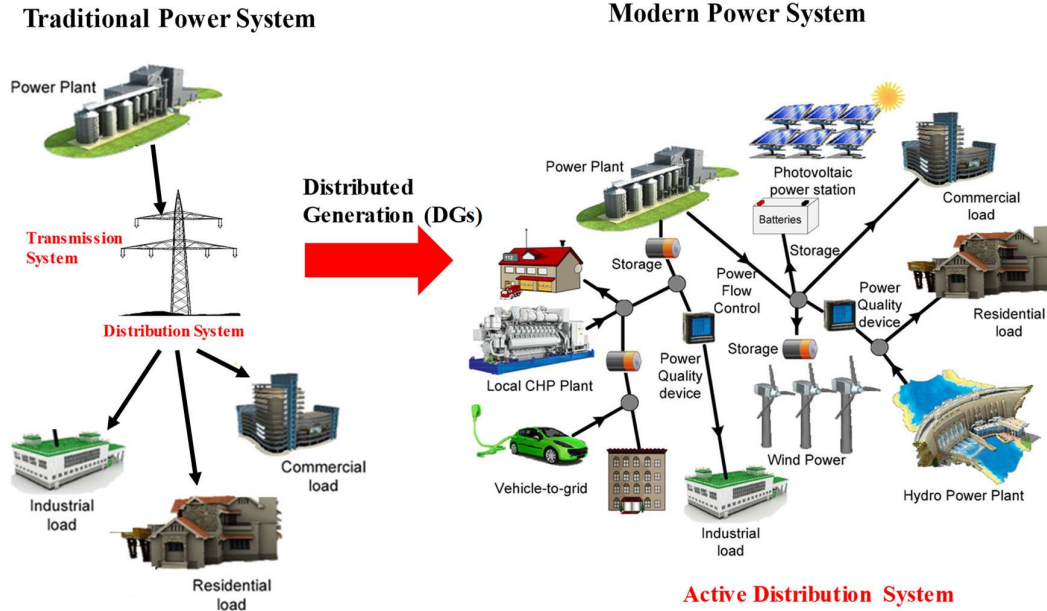


Figure 1.2 Traditional and active distribution system structures.

The centralized control methods coordinate voltage regulators by optimizing a certain objective, such as minimizing the voltage deviations and tap operations in DSs. The centralized control scheme is effective for the coordination among the DGs, OLTC, and SC. The approach can include day-ahead coordination [18], [19], management of the DG reactive power [20]–[22], voltage rise mitigation by coordination among battery energy storage systems (BESS) [23]–[26], microgrid voltage regulation [27], [28], and PV inverter reactive power control [29], [30]. These centralized control schemes can realize optimal control, whereas the high performance depends on the cost of the communication system, and its reliability against faults requires continued high investment.

The distributed control scheme relies on the independent decision of distributed controllers, where a coordination method is necessary to address the present voltage problems [31]. This strategy includes the off-line coordination of the parameters of conventional distributed controllers, and a multi-agent system (MAS) scheme that fully utilizes communications among them. There have been various works, such as the charge/discharge of BESS [32], controlling the DG active power generations [33], coordination among the OLTCs, SCs, and PV inverter reactive powers [34]–[36]. The

distributed approach is generally more reliable, since the individual controllers can act autonomously, even in the case of faults. However, the optimal performance cannot be achieved in general, except certain cases [37]–[39], where the optimality can be reached when the agents are allowed to communicate and cooperate.

Furthermore, different studies have been performed using the reactive power capability of the DGs in order to reduce the stress on the voltage control devices [14], [40], [41]. The reactive power devices have a fast response comparing with the traditional SVR or OLTC. Therefore, the reactive power capability of certain DG types, like PV, is used in several control methods to mitigate voltage regulation problems including voltage rise, voltage drop and voltage fluctuations [42]–[44].

Recently, the multi-agent system (MAS) has been used in a lot of studies to solve many voltage control problems in DSs. MAS is a control system composed of multiple agents, which can interact with each other and work together to solve problems based on the data collected by sensors, and it can act autonomously [45], [46]. The authors in [17] used the MAS to manage the power dispatch in the DS taking into account the uncertainty of DGs generation. A decentralized optimum control technique for the voltage regulation devices in DS has been proposed in [47]. This control method was formulated based on MAS to find the optimal setting for the voltage control devices in the DSs. In [16], a cooperative protocol based on MAS has been proposed, where the objective of this protocol is to minimize voltage deviation and mitigate the interference between tap regulators and DGs in active DSs

1.2 Research Objectives

Based on the above literature, considerable research work has been conducted to resolve the voltage control problems of the active DS. The main objective of this work is to develop effective voltage control schemes for DSs with high DGs penetration. This objective is achieved using the MAS architecture through the following sub-objectives:

1.2.1 Management of Voltage Regulators

In this thesis, an effective voltage control strategy for the voltage regulators in the unbalanced DS (UDS) is proposed [48]. The proposed method considers the features of the UDS and different types and configurations of voltage regulators. The difference of the proposed method from the existing methods lies in ensuring an optimal control action to minimize the voltage deviations in a simple manner without using a central controller. Furthermore, it is flexible to handle the possible changes in the DS topology and

operations of the PV systems using the distributed MAS scheme. The use of the MAS scheme yields a robust control performance in a flexible and reliable manner, even in the case of agent failure. The proposed method can optimally and effectively manage the voltage regulators in the UDS with an unbalanced PV distribution among the three-phases, decrease the device operation stresses and minimize the total voltage deviation. The proposed method can consider other conventional controllers (e.g., capacitors) to be operated as local controllers with their own setpoints.

1.2.2 Management of DGs Power

1.2.2.1 Reactive Power Control of DGs

A simple and effective management strategy is proposed for controlling the reactive power of the DGs using voltage/reactive power sensitivity analysis and MAS. The proposed strategy utilizes the reactive power capability of the DG sources to reduce the overall system voltage deviation. The proposed strategy represents each DG with its ability to supply or absorb reactive power as a control agent, and each DG have its own control parameter which is function of the local node voltage deviation and the voltage/reactive power sensitivity. The proposed method can simplify the coordination process among the different voltage regulation devices and the various DG sources in the DS to achieve an overall strategy for effective voltage control.

1.2.2.2 Active/Reactive Power Control of DGs Using Nodal Prices

A novel method is proposed for the management of the output power of the DGs in order to solve the voltage rise problem and the unfairness situation among the DGs generations. Two optimization problems are formulated: One is for the optimal operation of DS, where the objective is to maximize the total active power generations of the PVs subject to the voltage limits and PV inverter constraints. The other is for the individual PV prosumers to maximize their profits subject to the inverter constraints. An important thing is that the solutions of the both problems agree to each other by the following procedure: (1) The former optimization provides the nodal shadow prices of the active and reactive powers of PV inverter outputs; (2) Then prices are announced to the PV prosumers; and (3) The prosumers maximize their profit under the nodal prices. This method can also realize a fair profit situation among the prosumers, while maximizing total power generations and controlling the voltages within their limits. The voltage control in the proposed method is performed based on MAS described in [47]–[49],

where the information is exchanged via a common memory (blackboard memory) and each PV source acts as a control agent.

1.3 Thesis Outline

The thesis is organized as follows:

Chapter 1: presents the introduction to the active DSs, research objectives, scope of the research, and organization of the thesis.

Chapter 2: provides a comprehensive review of DS, impact of DGs on feeder voltage regulation, voltage control techniques, and MAS.

Chapter 3: presents an optimal voltage control strategy for voltage regulators in active UDS using MAS architecture. The proposed method is tested considering high PV penetration and compared with a conventional method. The simulation results demonstrate that the proposed strategy can effectively adjust the tap operations to minimize the voltage deviation with no tap oscillations under different sun profiles (sunny or cloudy).

Chapter 4: provides an effective control strategy for DGs reactive power based on MAS and voltage/reactive power sensitivity analysis. The proposed strategy utilizes the reactive power capability of the DG sources to reduce the overall system voltage deviation. The numerical results show that the proposed strategy can significantly mitigate voltage violation problems.

Chapter 5: provides a novel method for controlling photovoltaic (PV) power outputs for optimal operation of DS. The proposed method maximizes the total power of PVs in the DS by controlling their reactive power outputs while improving the voltage profiles. The results demonstrate that the proposed method is effective to mitigate the voltage violation problem and maximize the total PV power generations.

Chapter 6: provides a conclusion part, where contributions of the study are discussed. In addition, some recommendations for further research in the future are presented.

To give a unified picture and facilitate understanding the contents and the distribution of contributions among the different chapters Figure 1.3 is drawn, which describes the workflow in the thesis. According to the figure, the contents of the dissertation are divided into three parts, namely, Part I, Part II, and Part III.

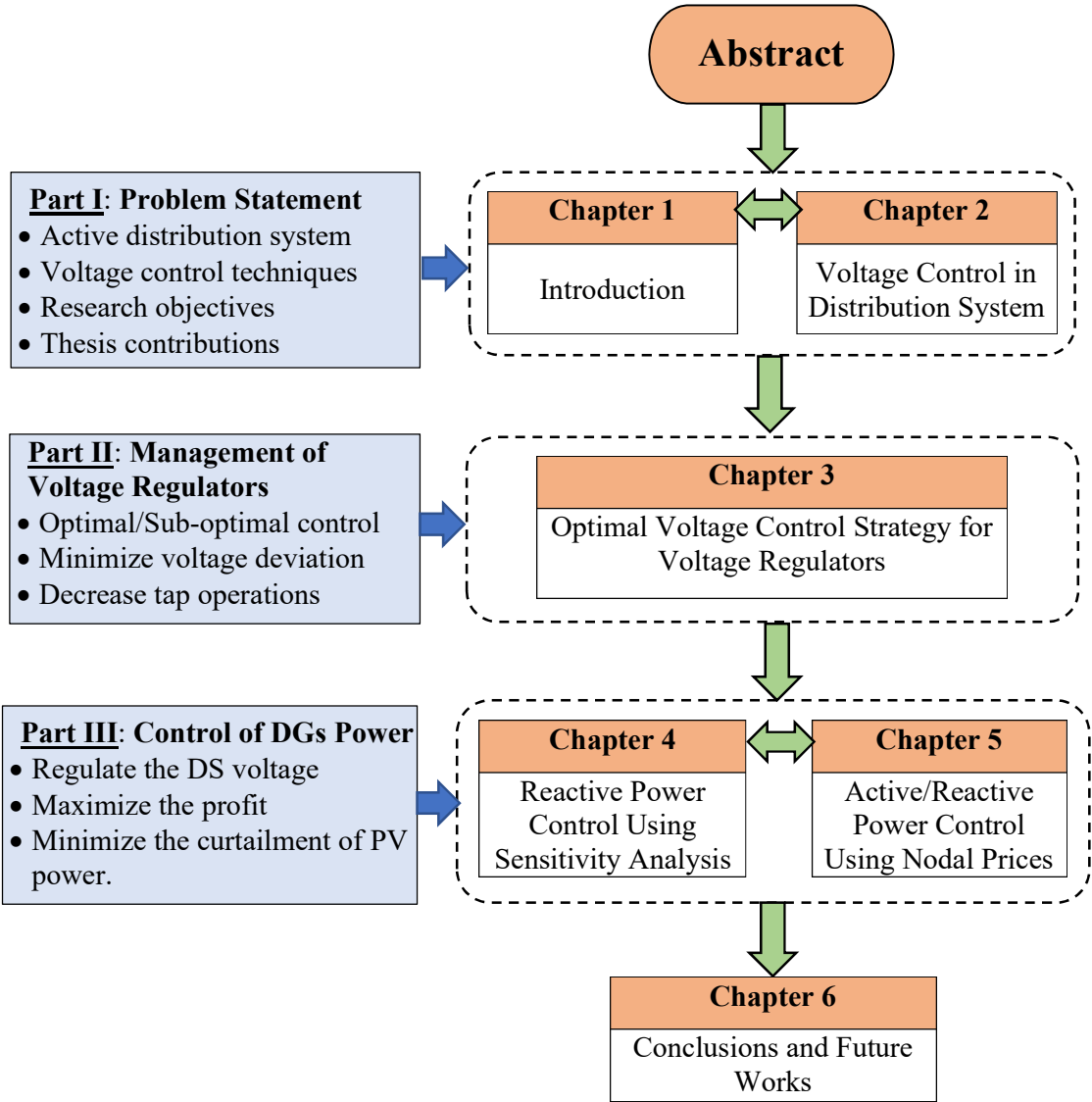


Figure 1.3 Structure of the thesis.

Chapter 2: Voltage Control in Distribution Systems

2.1 Introduction

This chapter presents a literature review on the voltage control in DS. The chapter starts with an introduction on the characteristics of the DS, the impact of DGs on feeder voltage regulation and network performance during different operating conditions. The chapter then focuses on the voltage control techniques. Lastly, a detailed explanation on the MAS and the voltage regulation using MAS architecture is described.

2.2 Distribution System Characteristics

The electrical DSs are an essential part of the electrical power system. In order to transfer electrical power from the transmission system to the place where it will be used by the consumers, some type of DSs must be utilized. The DSs are divided into two types, radial or meshed network. The radial structure of DSs makes the flow of the power in one direction from the source substation towards the customers and it is arranged like a tree where each customer has one source of supply. Radial systems are commonly used in rural or suburban areas. A network system has multiple sources of supply operating in parallel. In general, there are unique features, configurations, and characteristics of DSs which can be summarized as follows:

- Extremely large number of branches/nodes.
- Multiphase, unbalanced grounded or ungrounded operation.
- High R/X ratios.
- Three-phase transformers and voltage regulators.
- Unbalanced distributed load.
- High penetration of different types of DG technologies.

2.3 Impact of DGs on Feeder Voltage Regulation

Recently, the installation of different types of DGs in DS has increased rapidly. The traditional DS and their control strategies were designed based on the unidirectionally power flow scheme from the substation to the loads. The bidirectional power flow caused by the DGs generation changes the characteristics of the DSs from passive to active which can mislead the classic strategies of voltage control and cause various voltage

violations. The impact of the DG's presence on the DSs voltages can be illustrated as follows:

- **Overvoltage Problem:** The installation of the DG sources in the DSs, will affect the voltage regulation depending on the location, size, and operating scheme of the DG source. During high DGs generation and low load periods, there is a possibility of reverse power flow, which causes voltage rise, in the network as

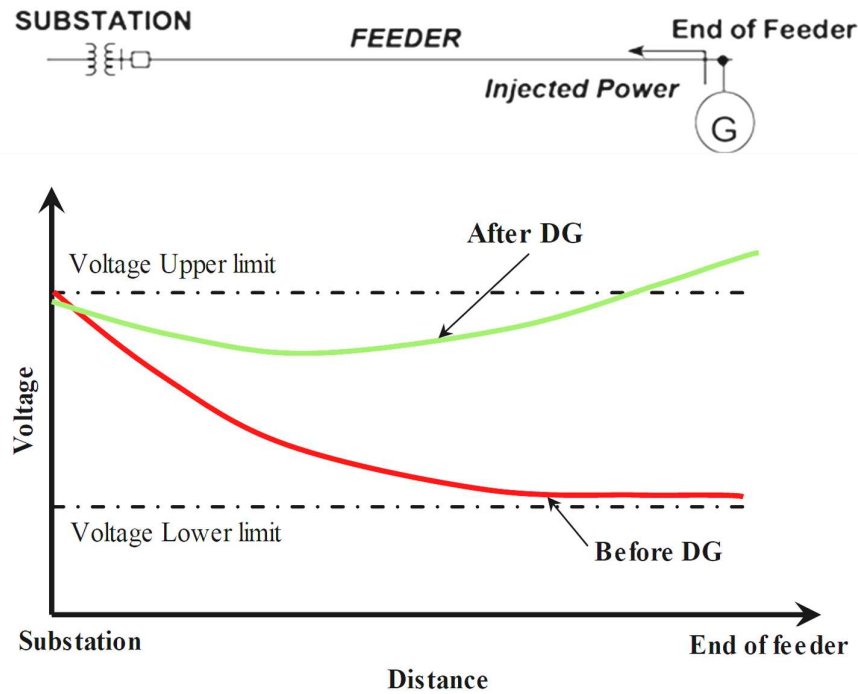


Figure 2.1 Voltage profile before and after addition of large DG.

shown in Figure 2.1 [50]. The overvoltage problem due to high DGs penetration restricts the DGs hosting capacity and increases the DGs power curtailment in the DS [51].

- **Voltage Fluctuations:** The varying output of renewable energy-based DG sources can cause voltage fluctuations on the feeder which lead to the oscillating of tap changers and capacitors. For example, the output power of wind turbines and PVs is highly dependent on weather conditions which are naturally random, these fluctuations will disturb the operation of the voltage control devices.
- **Interaction with the Voltage Control Devices:** The interaction of the voltage control devices and the DG sources affects the performance of the control devices and disturbs their conventional control strategies which increases the difficulties

to solve the voltage regulation problems. The fluctuated output of some DG sources like PV and wind generation systems because of their intermittent characteristics, increases the stress on the regulation devices, causes oscillations in the regulator tap, and affects the operation of the switched capacitors. Likewise, the DG that has feedback to regulate the voltage may interact negatively to the voltage control devices of the DS. Under such conditions, excessive cycling of voltage control devices can occur which will affect the power quality of the DS [52].

2.4 Voltage Control Techniques

All the devices, apparatus, electrical machines, consumer appliances etc. are all designed to be used within the standard voltage range. The variations of voltage in the DSs with different DG sources may affect the operation of those and cause performance deterioration. Therefore, it is desirable that the consumers receive power within the prescribed voltage limit. This section presents a comprehensive review of voltage control techniques for the active DSs, recommendations are provided in order to decrease the voltage violations and maximize the DGs utilization.

2.4.1 Tap Changing Transformers

The tap changing transformers (i.e. on-load tap changers (OLTCs), off-load tap changing transformers, and step voltage regulators (SVRs)) are the most common technique for voltage control in the DSs. It is an effective way to control the voltage by selecting the appropriate tap position. The standard step regulators can change the voltage by $\pm 10\%$ regulator range, usually in 32 steps.

There are various control characteristics associated with tap changing transformers such as:

- **Voltage level:** the voltage level to which the control will regulate (load center voltage).
- **Dead band or bandwidth:** the total voltage range around the voltage level which the control will consider acceptable.
- **Line drop compensation (LDC):** which set to compensate for the voltage drop between the regulator and the load center rather than at transformer terminals.
- **Time delay:** used to avoid taps oscillation during a transient or short time voltage fluctuations and it can be used to accommodate the operation of series and parallel regulators.

However, with increase the installation of DGs in the DSs, the performance of the tap changing transformers is affected, thus resulting in voltage regulation problems. Therefore, the regulators should have an effective and cooperative voltage control algorithm to overcome the voltage violations and keeps the voltage within the standard limits.

2.4.2 Shunt Capacitors (SC)

Shunt capacitor banks are important for the reliable operation of the DSs. The capacitor banks used to regulate voltage profiles and reduce reactive power flow through the power system.

Different approaches can be used to control the capacitor bank depending on the bank size, location, nearby capacitor bank, availability of the load tap changer (LTC), etc. these approaches can be described as follows [53]:

- *Voltage control*: the capacitor bank is controlled based on the measured node voltage.
- *Reactive power control*: the capacitor bank is controlled based on the measured reactive power.
- *Power factor control*: the capacitor bank is activated/deactivated according to the power factor limit.
- *Timed control*: the capacitor bank is activated/deactivated depending on the scheduled time (hour, day, month).
- *Manual control*: the capacitor bank is activated/deactivated manually based on needs.

2.4.3 Static Synchronous Compensator (STATCOM)

STATCOM is a shunt-connected FACTS device which can provide voltage control in either transmission or distribution system. The STATCOM generates/absorbs reactive power with a fast control response because no moving parts are used. The reactive output of the STATCOM is controlled to regulate the bus voltage with which it is connected. The STATCOM performs the voltage regulation in a more robust and flexible manner [54].

2.4.4 Energy Storage Systems (ESS)

The integration of energy storage systems (ESS) in the DSs can mitigate some of the problems of installing DGs with high penetration. The ESS can help in maximizing the

energy efficiency of the DS, improve the overall performance, mitigates the voltage deviation, and control the line losses [55]. Various types of ESS can be used in the DSs, i.e. fuel cells, flywheels Pumped hydro storage, compressed air energy storage (CAES), super-conducting magnetic energy storage (SMES), and the most widespread ESS are hydrogen and lead acid battery energy storage system (BESS) [56].

Various studies for voltage control have been performed using the EES, a coordinated control strategies for ESS with traditional voltage regulators (OLTC and SVR) and PV sources are proposed in [25], [26], [40], [57], [58]. The objective of the proposed methods is to regulate the voltage within the standard limits.

2.4.5 Network Reconfiguration

Network reconfiguration refers to reshape the distribution network topology by closing/opening the tie switches in order to optimize the system operations and achieve a certain objective such as system loss reduction, voltage stability, and voltage regulation [59], [60]. Although this technique is a new topic in voltage control for DSs with DG, some studies has been performed using the network reconfiguration to regulate the node voltages as described in [61]–[63].

2.4.6 Active/Reactive Power Control of the DGs

Voltage violations caused by the DG sources can be decreased by controlling active and reactive power of the DGs. The voltage can be regulated by reducing the DG active power generation or allowing the DGs which have the reactive power capability to absorb/inject reactive power to the network.

Active Power Curtailment of the DGs becomes a popular solution introduced in many voltage control schemes and it can be easily implemented with different type of DGs, i.e., biomass, hydro, wind turbines, and PV sources as illustrated in [50], [64], [65]. However, this method has a negative effect on the DG investment. Therefore, different approaches are proposed for managing the voltage regulation using the reactive power control of the DGs combined with the real power curtailment. Firstly, the DG absorb/inject reactive power until the constraints are reached. Then, If the reactive power control is not enough to regulate the voltage within the limits, the active power control strategy will used to regulate the voltage [56].

Recently, the PV inverter play an important role in the voltage regulation of the active DSs. Different techniques are proposed for the managing of active/reactive power of the PV inverter in order to control the voltage and mitigate the overvoltage problem [30],

[66]–[68]. These control techniques can be classified in two main approaches. The first one is a centralized control where the optimal active and reactive power are calculated using the optimal power flow (OPF) [69]–[71]. The second approach is a distributed control scheme where each PV inverter acts individually [34], [42]. Concerned with PV inverter control, the active power curtailment and the reactive power control of the PV power are major methods to mitigate the voltage rise problem in the DS. However, the management of PV power in DS may cause unfairness situation in the PV operations because the generated power is reduced in some specific PV nodes to reduce the voltage raise. Therefore, some control techniques are proposed to quantify this unfairness as described in [65], [72].

2.4.7 Cooperative Control Techniques

Recently, with increase the installation of different types of DG in the DS, using a single control technique becomes insufficient to solve the complicated voltage problems. Therefore, cooperative techniques and methodologies are widely used in the active DSs compared with the single control techniques. The coordination among the different control techniques has been developed in various research studies, a coordination between the reactive power compensation and the OLTC is proposed in [9], [16], [73]–[75]. Cooperative real-time control between PV inverters and BESS is proposed in [76]. In [77], a fast-acting approach is proposed to minimize the voltage deviations by determining the setting of regulator taps and the contributions of reactive power for both the capacitors and the DGs without active power curtailment.

2.5 Control Structures

Numerous control structures are used in the DS for the management of voltage control devices and it can be classified into centralized and distributed structures. The centralized control structure coordinates the voltage control devices by optimizing a certain objective using a central controller. The central controller collects and analyzes the network information and takes the control decisions and sends the control signal to the voltage control equipment. The centralized control scheme can provide the best performance for the coordination among the DGs, OLTC, SC, and smart inverters. But this scheme may become unpopular in the large DS for several reasons as follows:

- For high DGs penetration, the high performance requires large investments in the communication network.

- Large number of installed DGs with different size, type, and configuration.
- Increased the amount of uncertainties because of DG sources.
- Large computational burden is needed for network solution at each time step.

The distributed control structure depends on the autonomous decision of the voltage control devices based on the local information, where a coordination method is necessary to address the present voltage problems [31]. This strategy includes the off-line coordination of the parameters of conventional distributed controllers, and a multi-agent system (MAS) scheme that fully utilizes communications among them as described in the next section.

2.6 Multi-Agent System (MAS)

In recent years, with increase the integration of DGs in the DSs, the use of MAS is increased to control the system operation and solve the problems of the DSs [17], [78]. The MAS is a control system consisted of several controlled agents. The agent is a system which can take action and affects its environment based on the data collected by sensors, and it can acts autonomously [45],[46] . The independent agents need to cooperate with each other and coordinate their activities in order to avoid duplication of effort and achieves their goals in a simple manner [79].

The main advantages of the MAS can be described as follows:

- ***The ability to be extended:*** the number of agents can be easily extended.
- ***The flexibility:*** several agents with different abilities can work together to achieve a desired goal.
- ***The Robustness:*** the ability to act even in case of communication failure.
- ***The fast response:*** the agents can work simultaneously to achieve a goal.

2.6.1 MAS Architectures

The MAS system consists of several control agents, the agents can coordinate together to achieve the desired goal with different communication methods. As shown in Figure 2.2, two main strategies can be used to for exchange information among agents as follows [80]:

- 1) The agent can exchange information directly to a specific agent or all agents or specific group of agents
- 2) The agent can access a shared data in a common memory (referred to as a blackboard) in which information can be posted and read by the other agents.

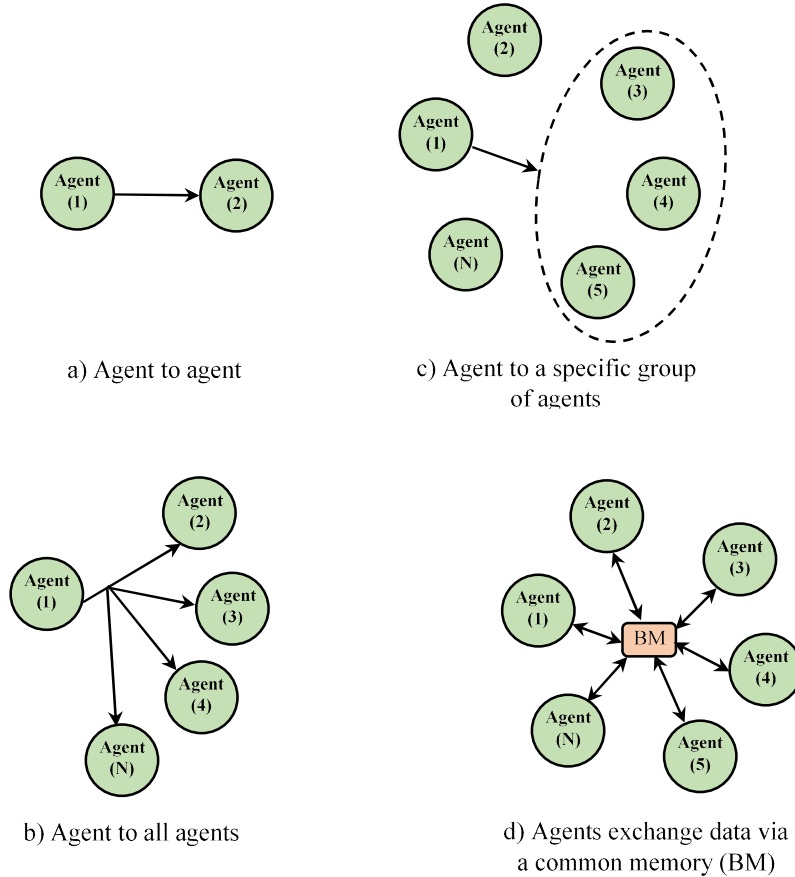


Figure 2.2 Basic communication in the MAS [80].

Also, some literature classifies the MAS architecture to centralized, distributed and hierarchical control system as described as in the following [31], [81].

1) The centralized approach

- The local agents send their local information to the control center as shown in in Figure 2.3.
- The control center takes the decisions and sends the control signal to the local agents.
- The local agents act based on the control signal in order to achieve the desired goal.

The performance of the centralized control method is affected by the reliability and the speed of the employed communication system. This mean that the high performance operation will be costly and more complicated to overcome the communication failure and increase the overall system efficiency [82]-[83].

2) The hierarchical approach

In this approach, the agents are working in different levels of decision making as shown in Figure 2.4 . The control center is at the head of the system which represent the high level of control and it decides and send the appropriate control signal based on the collected information from the lower level agent. The agents at the lower level are responsible for collecting information from the lower agents and pass control signal. In this approach, only the higher-level agents are responsible for decision-making and the lower level agents can only able to communicate with higher level agents. The main disadvantage of this approach is that the failure of higher-level agents can critically affect all lower level agents

3) The Distributed approach

The distributed control approach relies on the independent decision of distributed agents. In the distributed approach there is no central controller, the agents share the information each other to reach the goal. This nature of distributed MAS control reduces communication. The decentralized systems are more powerful and adaptable as opposed to the centralized ones however, the optimal performance cannot be achieved in general. The control center is simply considered as a supervisory observing. In some cases, the control center additionally considered as a part of decision making.

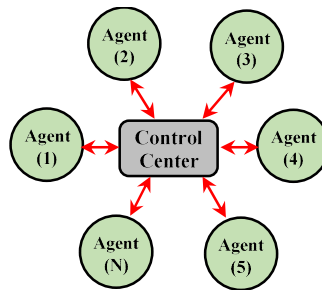


Figure 2.3 Centralized MAS architecture.

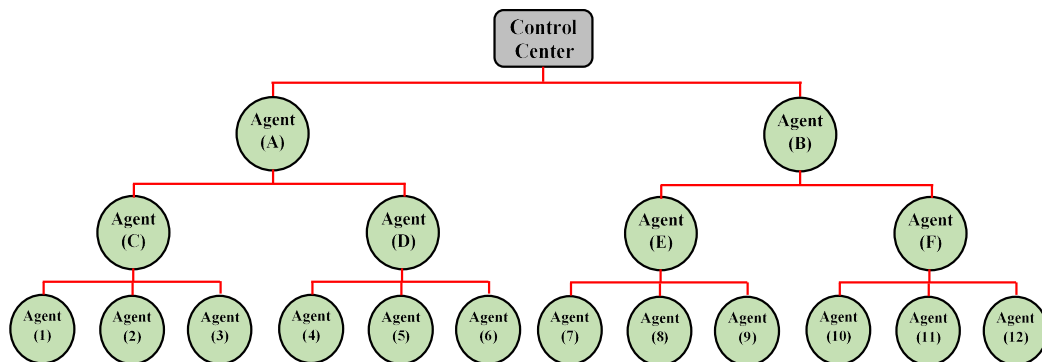


Figure 2.4 Hierarchical MAS architecture.

2.6.2 MAS for Feeder Voltage Regulation

Recently, The MASs have been used to solve many problems in the electric power network and are being developed for a range of applications.

Various studies have been performed for the voltage regulation in the active DS using the MAS architecture. The MAS is used to control the traditional voltage regulators in order to decrease the voltage violations and decrease tap oscillations of the transformers in [13], [47], [48], [84]. A cooperative strategies has been proposed in [14], [16] for active DS using the MAS where OLTC and DG units are considered as control agents. The objectives of the study are the minimizing of the voltage deviation, reducing the tap operation, eliminate the feeders' congestion and maximizing the energy of DG units. Also, in [72], [85] the MAS is used to manage the active and reactive power of the PV sources in order to regulate the voltages within standard limits and realize a fair profit situation among the prosumers, while maximizing total power generations.

2.7 Summary

The voltage control in DS with high DG penetration is an important and challenging issue for the system operator, DG owners and customers. This chapter focused on providing some facts about the main features of distribution systems, the impact of DGs on voltage regulation, the different techniques of voltage control, and the MAS for voltage regulation. Based on these literature, effective strategies are proposed in this thesis to regulate the voltage of the active DSs.

Chapter 3: Optimal Control Strategy for Voltage Regulators in Active UDS

3.1 Introduction

This chapter presents an effective control strategy for voltage regulators in the DS based on the voltage sensitivity using MAS architecture. The features of the UDS with DGs and different types and configurations of voltage regulators are considered in the proposed strategy. The novelty of the proposed method lies in realizing both the control optimality of minimizing voltage violations and the flexibility to accommodate changes in the DS topology using an MAS scheme. An advantageous feature of using the MAS scheme is the robust control performance in normal operation and against system failure. Simulation studies have been conducted using IEEE 34-node and 123-node distribution test feeders considering high PV penetration and different sun profiles. The results show that the proposed voltage control strategy can optimally and effectively manage the voltage regulators in the UDS, which decrease their operation stresses and minimize the overall voltage deviation.

3.2 Proposed Control Strategy

3.2.1 Proposed MAS Control Strategy for the UDS

The construction of the DS includes unbalanced loads, unbalances in lines, single-phase or three-phase DG sources, and different configurations of voltage regulation devices. Therefore, a UDS can be represented as an MAS consisting of different agents. Each voltage regulator will act as a control agent that works autonomously according to the data received from the blackboard memory (BM). The BM is used to achieve the optimality of the control objective.

The proposed MAS architecture is illustrated in Figure 3.1 for the UDS, and it has the following features:

- Each agent receives information from two sources: measurements from its own area and from the BM.
- Each agent can calculate its own control parameter (referred to as index S in this paper) based on the obtained information.

The BM collects information from all agents, and each agent recognizes the status of the other agents through this information.

- Each agent takes action according to the received information from the BM to minimize an objective.
- In case of a communication failure, each agent can optimally control itself to achieve its desired goals based on the available data.

A management agent can be useful for system monitoring and real-time calculation, while the proposed method can autonomously work and optimally perform without using it. The optimality of the proposed method is explained in the Appendix B.

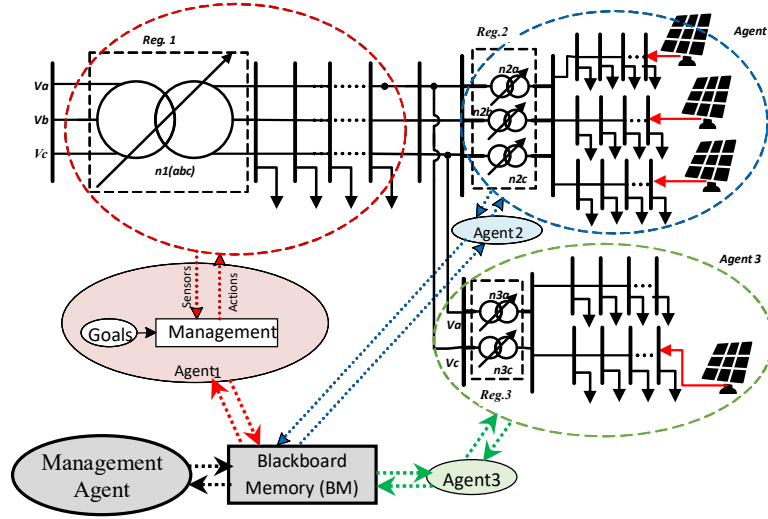


Figure 3.1 Proposed MAS for the UDS.

3.2.2 Optimal voltage control strategy

The optimality is realized each time by selecting the most effective controller (k) in the set of all discrete control parameters (K) to reduce the absolute value of the total voltage deviations in the system. The objective is to minimize (1).

$$\min_{k \in K} \int_0^{\infty} VD_{abc}(\mathbf{v}) dt, \quad VD_{abc}(\mathbf{v}) \geq 0 \quad (3.1)$$

In this formula, VD_{abc} is the positive three-phase voltage deviation function, which is defined as the sum of the voltage deviations at all observation points in the DS from the reference values. Since UDSs can have different line configurations, including star and delta, the voltage deviation function consists of the voltages in the DS with all line configurations as follows:

$$\begin{aligned}
 VD_{abc}(\mathbf{v}) &= \underbrace{VD_a(\mathbf{v}) + VD_b(\mathbf{v}) + VD_c(\mathbf{v})}_{Yconfig.} + \underbrace{VD_{ab}(\mathbf{v}) + VD_{bc}(\mathbf{v}) + VD_{ca}(\mathbf{v})}_{\Delta config.} \\
 &= \frac{1}{2} \sum_{Y=a}^c \sum_{j=1}^{M_Y} w_j^Y \cdot (v_j^Y - v_{Rj}^Y)^2 + \frac{1}{2} \sum_{\Delta=ab}^{ca} \sum_{i=1}^{M_\Delta} w_i^\Delta \cdot (v_i^\Delta - v_{Ri}^\Delta)^2
 \end{aligned} \tag{3.2}$$

For Y-connected regions:

- VD_a , VD_b , and VD_c are the voltage deviation functions for phases a, b, and c, respectively.
- v_j^Y is the voltage at node j phase Y ($Y = a, b, c$).
- w_j^Y is the weight coefficient of node j phase Y .
- v_R^Y is the reference value of the phase voltage.

For Δ -connected regions:

- VD_{ab} , VD_{bc} , and VD_{ca} are the voltage deviation functions for lines ab , bc , and ca , respectively.
- v_i^Δ is the line voltage at node i , and ($\Delta = ab, bc, ca$).
- w_i^Δ is the weight coefficients of node i line Δ .
- v_R^Δ is the reference value of the line voltage.

The weight coefficients in (3.2) can be considered indicators of the importance of individual observation points. The constraints of minimization (3.1) are the power flow equations (3.3) and those for the tap operations, which will be provided in the next section.

3.3 Control Method Formulation

3.3.1 Mathematical formulation

The voltages in the UDS are governed by the power flow equations, and they are the function of the tap positions of voltage regulators n , and the load parameters L are described in (3.3).

$$\mathbf{v} = \mathbf{f}(\mathbf{L}, \mathbf{n}) \tag{3.3}$$

where, $\mathbf{v} = [v_1, v_2, \dots, v_M]^T$, $\mathbf{n} = [n_1, n_2, \dots, n_N]^T$ and $\mathbf{L} = [L_1, L_2, \dots, L_p]^T$.

Since the proposed method depends on controlling the voltage regulator taps to minimize the overall voltage deviation, the next tap position of regulator k , $n_k^p(t+1)$ is a control parameter, which can be expressed as follows:

$$n_k^p(t+1) = n_k^p(t) + \Delta n_k^p(t), \quad n_{k,\min}^p \leq n_k^p \leq n_{k,\max}^p$$

$$\text{where, } p \in \begin{cases} a, b, c & \text{for Y connected regulators} \\ ab, bc, ca & \text{for } \Delta \text{ connected regulators} \end{cases} \quad (3.4)$$

The tap change in regulator k at time t is described by $\Delta n_k^p(t)$, and it depends on the regulator step size and tap status, which can be expressed as follows:

$$\Delta n_k^p(t) = R_k^p \cdot Z_k^p(t), \quad Z_k^p(t) = \begin{cases} +1 & \text{(tap increase)} \\ 0 & \text{(no tap change)} \\ -1 & \text{(tap decrease)} \end{cases} \quad (3.5)$$

where R_k^p and $Z_k^p(t)$ are the step size and tap status of regulator k phase or line p , respectively.

According to (3.3), the change in the objective is given as

$$\begin{aligned} \Delta VD_{abc}(\mathbf{v}(t)) &= VD_{abc}(\mathbf{v}(t+1)) - VD_{abc}(\mathbf{v}(t)) \\ &= \left[\frac{\partial VD_{abc}}{\partial \mathbf{v}} \right] \cdot \left[\frac{d\mathbf{v}}{d\mathbf{n}} \right] \cdot \Delta \mathbf{n}(t) \end{aligned} \quad (3.6)$$

Equation (3.6) can be written as follows:

$$\begin{aligned} \Delta VD_{abc}(t) &= \left[\frac{\partial VD_{abc}}{\partial \mathbf{v}} \right] \cdot \left[\frac{d\mathbf{v}}{d\mathbf{n}} \right] \cdot \mathbf{R} \cdot \mathbf{Z}(t) \\ &= \mathbf{S}_{abc}(t) \cdot \mathbf{Z}(t) = \sum_{k=1}^N S_{k(abc)}(t) \cdot Z_k(t) \\ &= \underbrace{\sum_{y=a}^c \sum_{j=1}^{N_y} S_j^y(t) \cdot Z_j^y(t)}_{Yconfig.} + \underbrace{\sum_{x=ab}^{ca} \sum_{i=1}^{N_x} S_i^x(t) \cdot Z_i^x(t)}_{\Delta config.} \end{aligned} \quad (3.7)$$

where

$$\mathbf{Z}(t) = [Z_1(t), Z_2(t), \dots, Z_N(t)]^T \text{ and } \mathbf{R}(t) = \text{diag}[R_1(t), R_2(t), \dots, R_N(t)].$$

$\mathbf{S}_{abc}(t)$ is the sensitivity of the objective with respect to the unit change in the regulator taps; therefore, $\mathbf{S}_{abc}(t)$ can be used as an index for optimal control to find the most effective controller. The index can be computed as follows:

$$\begin{aligned}
 \mathbf{S}_{abc}(t) &= \left[\frac{\partial VD_{abc}}{\partial \mathbf{v}} \right] \cdot \left[\frac{d\mathbf{v}}{d\mathbf{n}} \right] \cdot \mathbf{R} = \underbrace{\sum_{y=a}^c \sum_{j=1}^{N_y} S_j^y(t)}_{Y \text{ Regulators}} + \underbrace{\sum_{x=ab}^{ca} \sum_{i=1}^{N_x} S_i^x(t)}_{\Delta \text{ Regulators}} \\
 &= [S_1(t), S_2(t), \dots, S_N(t)].
 \end{aligned} \tag{3.8}$$

where $[d\mathbf{v}/d\mathbf{n}]$ is the voltage/tap sensitivity matrix calculated by (3). N_y and N_x are the number of phase and line voltage regulators for the star and delta configurations, respectively.

An optimal control to minimize the objective can be realized using the three-phase index S as follows.

$$\min_{k \in K} VD_{abc}(\mathbf{v}(t+1)) = VD_{abc}(\mathbf{v}(t)) + \min_{k \in K} \{ \mathbf{S}_{abc}(t) \cdot \mathbf{Z}(t) \} \tag{3.9}$$

3.3.2 Proposed Control Rules

➤ *For optimal operation*

The proposed strategy can perform an optimal operation for the UDS by calculating only index S in each control agent. If the index values are shared among agents, each agent can independently take its control action. According to (3.9), the agent with the highest value of index S should change its regulator taps as follows:

$$\begin{aligned}
 S_k^p(t) &= \max [|S_1^p(t), \dots, S_N^p(t)|] > \alpha \\
 &= \max_i |S_i(t)| > \alpha
 \end{aligned} \tag{3.10}$$

where α is a threshold value, $i \in K = \{1, \dots, N\}$, and N is the number of system regulators.

Tap k will change according to the following.

$$\begin{aligned}
 \text{if } |S_k^p(t)| &= \max_{i,p} |S_i^p(t)| \quad \text{and } S_i^p(t) < -\alpha \quad \text{then } Z_k^p(t) = 1 \\
 \text{if } |S_k^p(t)| &= \max_{i,p} |S_i^p(t)| \quad \text{and } S_i^p(t) > \alpha \quad \text{then } Z_k^p(t) = -1 \\
 \text{if } |S_k^p(t)| &\neq \max_{i,p} |S_i^p(t)| \quad \text{then } Z_k^p(t) = 0
 \end{aligned} \tag{3.11}$$

In the optimal control strategy, each agent should know the index S values of the other agents. At each time t , the values of the indices are compared, and the controller with the highest value is activated as described in (3.11). This action ensures that the agents minimize the overall voltage deviation and local voltage deviations of the violated area.

The proposed control strategy described in (3.10) and (3.11) can be useful even in the conventional centralized control scheme.

➤ **For suboptimal operation**

The proposed suboptimal scheme is to avoid the comparison process among the values of indices of the other agents. We propose that each agent performs control by its own index S when it is greater than a predefined threshold as below.

$$\begin{aligned}
 \text{if } S_k^p(t) < -\alpha_0 & \quad \text{then } Z_k^p(t) = 1 \\
 \text{if } S_i^p(t) > \alpha_0 & \quad \text{then } Z_k^p(t) = -1 \\
 \text{if } |S_k^p(t)| < \alpha_0 & \quad \text{then } Z_k^p(t) = 0
 \end{aligned} \tag{3.12}$$

where $\alpha_0 \geq \alpha \geq 0$.
 $\alpha_0 \neq 0$

Threshold α_0 is a common value among all controllers. This treatment expects that only one controller reacts at a time, which implies the optimal action. The suboptimal control strategy can be used even in the normal condition. In this case, each agent can act independently as a decentralized control system according to (3.12). This strategy is suitable for autonomous control but does not guarantee strict optimality (See Appendix B). The suboptimal strategy is useful when the data from the other agents are not fully available or reliable. If an agent fails to know the index S values of other agents because of communication loss or any abnormal conditions, it will act based on its own measurements.

The threshold values (α and α_0) in (3.11) and (3.12) are used as tuning factors that determine the amount of voltage deviation that causes the taps to take actions. Therefore, the threshold values (α and α_0) are useful to adjust the response time of the controllers. A large value admits a large voltage deviation, which implies that the responses of the controllers become slow and vice versa. The threshold value can be set by the system operator.

3.3.3 Formula of Index S

Based on (3.8) and (3.9), index S for regulator k is written as follows:

$$\begin{aligned}
 S_k^p(t) &= r_k^p \cdot \sum_p \sum_{j=1}^{M_{kp}} \frac{VD_{abc}}{\partial v_j^p} \cdot \frac{dv_j^p}{dn_k^p} \\
 &= r_k^p \cdot \sum_p \sum_{j=1}^{M_{kp}} w_j^p \cdot (v_j^p - v_R) \cdot \frac{dv_j^p}{dn_k^p}
 \end{aligned} \tag{3.13}$$

where M_{kp} is the number of observation nodes for the area of regulator k .

The voltage/tap sensitivity matrix $[dv/dn]$ is an important term in the computation of three-phase index S as in (3.13). It is a possible strategy that the accurate real-time calculation of the voltage/tap sensitivity matrix is performed on-line by the management agent based on the power flow computation using (3.3). In this case, the proposed method is effective for any networks including the meshed configuration. However, to reduce the computational burden of the control process, a simplified method for radial networks is proposed in the next section.

3.4 Formulation of Voltage/tap Sensitivity Matrix

The voltage/tap sensitivity matrix can be approximated based on only the network configuration assuming that all transformers are ideal [47], [86]. The voltage/tap sensitivities for different types of regulators and system configurations are given as follows:

3.4.1 Single-phase Regulators

The approximate values for the voltage/tap sensitivity matrix for the single-phase regulator are described in (3.14).

$$\frac{\partial v_{Hk}}{\partial n_k} = 0, \quad \frac{\partial v_{Gk}}{\partial n_k} = 1 \quad (3.14)$$

where G is the set of system nodes that can be affected by changing tap k (downstream nodes), and H is the other nodes that are not affected by changing the tap (upstream nodes).

3.4.2 Three-phase Star Connected Regulators

The three-phase star connected regulators can be classified into two categories as follows:

3.4.2.1 Three Taps Ganged Together

In this type, the three taps simultaneously change; therefore, they can be modeled as one controller, as described in (3.15) and (3.16).

$$n_a = n_b = n_c = n_{k(abc)} \quad (3.15)$$

The voltage/tap sensitivity matrix is as follows:

$$\frac{dv_{Gk(abc)}}{dn_{k(abc)}} = \begin{pmatrix} \frac{\partial v_{ka}}{\partial n_{k(abc)}} \\ \frac{\partial v_{kb}}{\partial n_{k(abc)}} \\ \frac{\partial v_{kc}}{\partial n_{k(abc)}} \end{pmatrix} = \begin{pmatrix} 1 \\ 1 \\ 1 \end{pmatrix} \quad (3.16)$$

3.4.2.2 Three Independently Controlled Regulators

In this type, the tap of each phase can change separately, which is modeled as three independent regulators. The voltage/tap sensitivity matrix for this type of regulators is as follows:

$$\frac{\partial v_{Gk(a,b,c)}}{\partial n_{k(a,b,c)}} = \begin{pmatrix} \frac{\partial v_{ka}}{\partial n_{ka}} & \frac{\partial v_{ka}}{\partial n_{kb}} & \frac{\partial v_{ka}}{\partial n_{kc}} \\ \frac{\partial v_{kb}}{\partial n_{ka}} & \frac{\partial v_{kb}}{\partial n_{kb}} & \frac{\partial v_{kb}}{\partial n_{kc}} \\ \frac{\partial v_{kc}}{\partial n_{ka}} & \frac{\partial v_{kc}}{\partial n_{kb}} & \frac{\partial v_{kc}}{\partial n_{kc}} \end{pmatrix} = \begin{pmatrix} 1 & 0 & 0 \\ 0 & 1 & 0 \\ 0 & 0 & 1 \end{pmatrix} \quad (3.17)$$

where n_{ak}, n_{bk}, n_{ck} are taps a, b and c, respectively, for regulator k . The number of independent taps in (3.17) vary with the existing phases.

3.4.3 Three-Phase Delta Connected Regulators

3.4.3.1 Closed Delta

The voltage equations for closed delta regulators in [7] is used to derive the approximated voltage/tap sensitivity matrix as follows:

$$\frac{\partial v_{Gk(ab,bc,ca)}}{\partial n_{k(ab,bc,ca)}} = \begin{pmatrix} \frac{\partial v_{kab}}{\partial n_{kab}} & \frac{\partial v_{kab}}{\partial n_{kbc}} & \frac{\partial v_{kab}}{\partial n_{kca}} \\ \frac{\partial v_{kbc}}{\partial n_{kab}} & \frac{\partial v_{kbc}}{\partial n_{kbc}} & \frac{\partial v_{kbc}}{\partial n_{kca}} \\ \frac{\partial v_{kca}}{\partial n_{kab}} & \frac{\partial v_{kca}}{\partial n_{kbc}} & \frac{\partial v_{kca}}{\partial n_{kca}} \end{pmatrix} = \begin{pmatrix} 1 & 1 & 0 \\ 0 & 1 & 1 \\ 1 & 0 & 1 \end{pmatrix} \quad (3.18)$$

where $n_{kab}, n_{kbc}, n_{kca}$ are the taps of lines ab, bc, and ca, respectively, for regulator k . As observed from (18), the change in a single tap will affect the voltages in two phases.

3.4.3.2 Open Delta

In this type of regulator configuration, two single-phase regulators are connected between two phases. The voltage/tap sensitivity matrix for the two single-phase regulators connected between phases AB and CB is expressed in (3.19).

$$\frac{\partial v_{Gk(a,b,c)}}{\partial n_{k(a,b,c)}} = \begin{pmatrix} \frac{\partial v_{kab}}{\partial n_{kab}} & \frac{\partial v_{kab}}{\partial n_{kbc}} & \frac{\partial v_{kab}}{\partial n_{kca}} \\ \frac{\partial v_{kbc}}{\partial n_{kab}} & \frac{\partial v_{kbc}}{\partial n_{kbc}} & \frac{\partial v_{kbc}}{\partial n_{kca}} \\ \frac{\partial v_{kca}}{\partial n_{kab}} & \frac{\partial v_{kca}}{\partial n_{kbc}} & \frac{\partial v_{kca}}{\partial n_{kca}} \end{pmatrix} = \begin{pmatrix} 1 & 0 & 0 \\ 0 & 1 & 0 \\ 1 & 1 & 0 \end{pmatrix} \quad (3.19)$$

3.5 Control Procedure

The proposed control algorithm for each agent is illustrated in Figure 3.2, which is explained as follows:

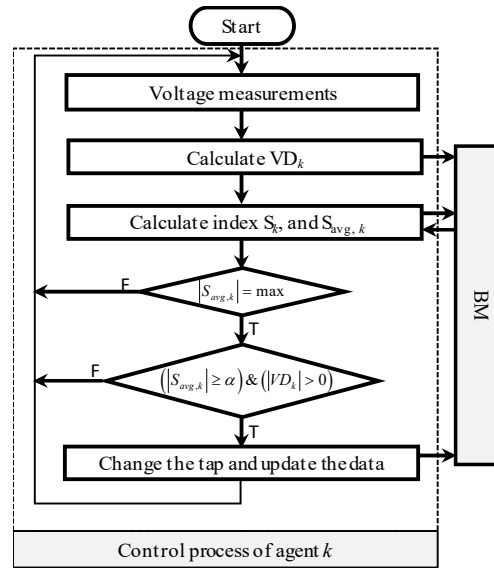


Figure 3.2 Proposed voltage control method.

3.5.1 Agent Measurement Process

In this stage, the agent measures the present tap position and voltages of the observation points in its monitoring area.

3.5.2 Agent Calculation Process

Based on the measurements, the agent will calculate the following parameters:

- *Center voltage*: The minimum and maximum voltage values are identified to compute the center voltage as follows.

$$vc_k^p = \frac{v_{k \min}^p + v_{k \max}^p}{2} \quad (3.20)$$

where $v_{k \min}^p$ and $v_{k \max}^p$ are the minimum and maximum voltages, respectively, at phase or line p of area k as shown in Figure 3.3.

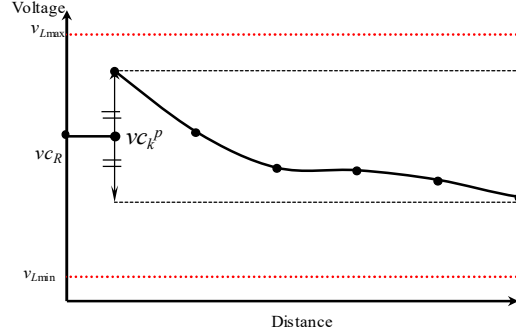


Figure 3.3 Utilized voltage control parameters in area k.

- *Voltage deviation*: The deviation of the center voltage from its reference value is calculated as follows:

$$VD_k^p = (vc_k^p - \max(d, vm_k^p) - vc_R) \quad (3.21)$$

$$vm_k^p = \left[\frac{v_{k \max}^p - v_{k \min}^p}{2} \right] - \left[\frac{v_{L \max} - v_{L \min}}{2} \right] \quad (3.22)$$

$$vc_R = \frac{v_{L \min} + v_{L \max}}{2} \quad (3.23)$$

where $v_{L \min}$ and $v_{L \max}$ are the standard minimum and maximum voltage limits, and d is a small positive value that acts as a dead band. The dead band (d) is adjusted by the operator based on the system condition and is a function of nominal voltage, where the value is $\pm 1\%$ of the nominal voltage in this study.

- *Index S*: Three-phase index S is calculated using (3.13).
- *Moving average of index S*: To ensure a smoothed control action, the time series moving average of index S is calculated using (3.24).

$$S_{avg,k}^p = \frac{1}{n} \sum_{j=1}^n S_k^p \quad (3.24)$$

3.5.3 Agent Data Collection

The agent sends the voltage deviation of (3.21) and average values of index S of (3.24) to the BM. (When the data are accepted by the BM, the BM will classify the status of each agent data as “1” for updated data and “0” for old data).

3.5.4 Agent Control Action:

The agent reads the BM data for the other agents and takes action. The action will differ according to the agent data status as follows:

Optimal action: When all agents work normally, the own index S is maximum compared with the others, and the tap is within limits, the agent initiates the control action according to (3.10) and (3.11).

Suboptimal action: The agent initiates the control action when the tap is within limits and the own index S is greater than the presetting threshold value according to (3.12). This case is useful under system fault. This situation may be identified from the status of the other agent data.

It is noted that the proposed suboptimal control process can easily be completed by only the individual agents without the interaction of the central management agent, since it avoids the comparison process of the indices. Nevertheless, the optimal control performance is realized as shown in Figure 3.13 and the Appendix B.

3.6 Results and Discussion

In this section, different case studies are conducted to evaluate the overall performance of the proposed control strategy. The maximum and minimum system voltages limits used for the simulation are 1.05 p.u. and 0.95 p.u., respectively. All measurements are equally weighted in (3.2). Two IEEE test systems are used in this study as follows:

3.6.1 IEEE 123-node Test Feeder

The IEEE 123-node test feeder in Figure 3.4 represents the UDS characterized by

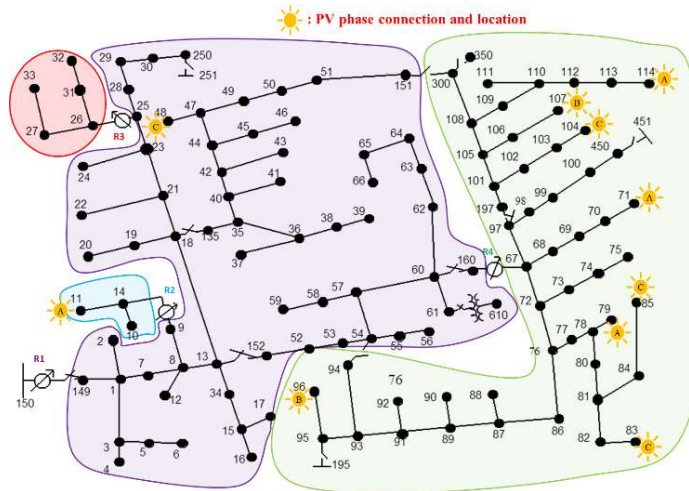


Figure 3.4 IEEE 123-node test feeder.

unbalanced loading and four voltage regulators with different configurations as illustrated in Table 3.1 [87]. The feeder is classified into four areas; each area can act as a control agent.

The total daily active and reactive power of loads and PV output (Clear and cloudy day) are shown in Figure 3.5. The locations of the PV sources and the system configuration are illustrated in Figure 3.4.

Table 3.1 IEEE 123-node test feeder regulator data

Reg. ID	Line segment	Phases	Configuration
1	150-149	A-B-C	3-Ph wye, gang operated
2	9-14	A	1-Ph, line-to-neutral connected
3	25-26	A-C	Two 1-Ph, open wye connected
4	160-67	A-B-C	Three 1-Ph, wye connected

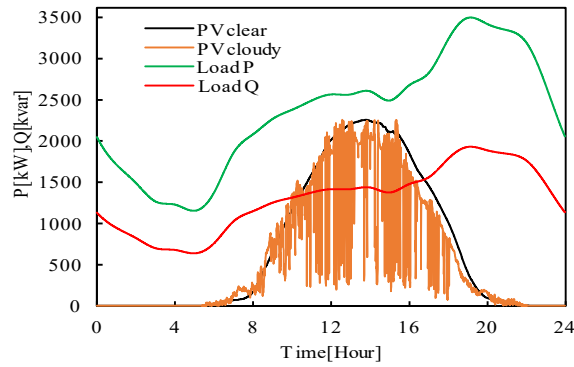


Figure 3.5 Total active and reactive power of the loads and PV.

3.6.1.1 Case Studies

Four cases are investigated to study different scenarios for the PV and network. The investigation is summarized in Table 3.2. In this study, we use $\alpha = 2.45 \times 10^{-7}$ and $\alpha_0 = 3.5 \times 10^{-7}$ for optimal and suboptimal controls. The simulation cases will be discussed below:

1) Case C0: Without control

a) Clear day condition

This case illustrates the voltage problems that occur in different regions of the IEEE 123-node test feeder during the clear day of PV as shown in Figure 3.5. As illustrated in Figure 3.4 and described in Table 3.1, the system is divided into four regions with different regulator configurations.

Figure 3.6 illustrates the maximum voltage deviation in the area of regulator no. 4, where the voltage rise problem occurs in phase (c) feeder during the PV peak time due to high PV penetration. Simultaneously, a voltage drop problem appears in phase (a) between hour 11 and 23; the area of three-phase regulator no. 1 also has a voltage drop problem between hour 17 and 22.

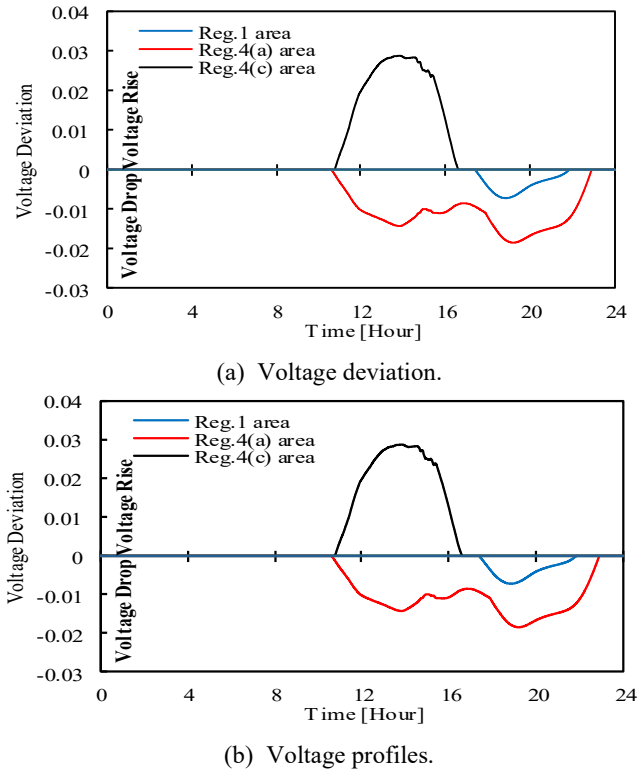
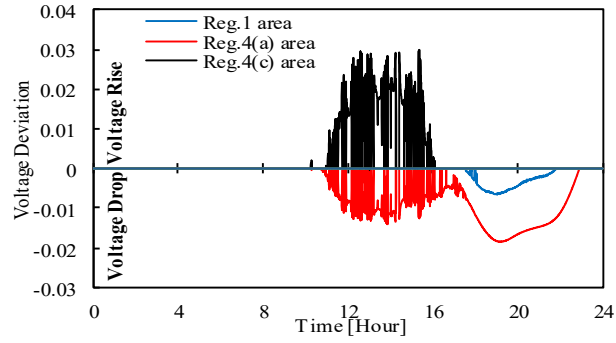


Figure 3.6 Results of Case 0: Without control for the clear day.

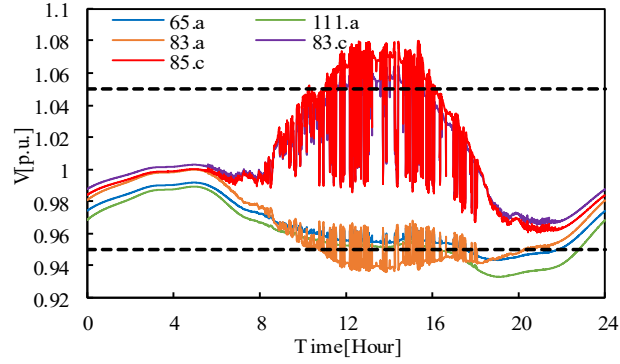
b) Cloudy day condition

As shown in Figure 3.7 (a), voltage fluctuations with voltage rise and voltage drop problems occur at the peak time of PV power in the area of regulator no. 4 in phases (a) & (c) (nodes 85, 83 and 111). The voltage profile in Figure 3.7 (b) illustrates that the area of three-phase regulator no. 1 has a voltage drop problem during hours 17 and 22.

Figure 3.7 (b) illustrates the voltage profiles of the nodes at which the large voltage deviations occur; the maximum voltage rise occurs in the area of regulator no. 4 in phase (c) feeder at nodes 83 and 85. The voltage profiles of nodes 65, 111, and 83 show that the maximum voltage drop occurs at phase (a) for the areas of regulators no. 1 and no. 4.

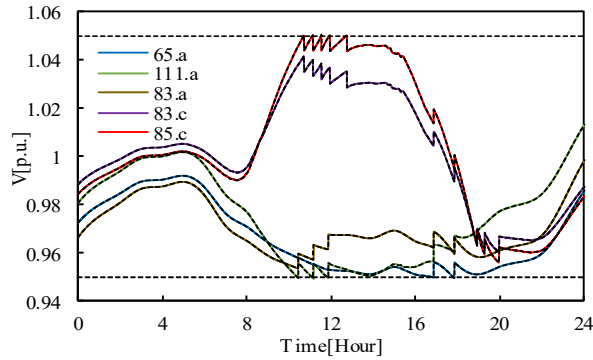


(a) Voltage deviation.

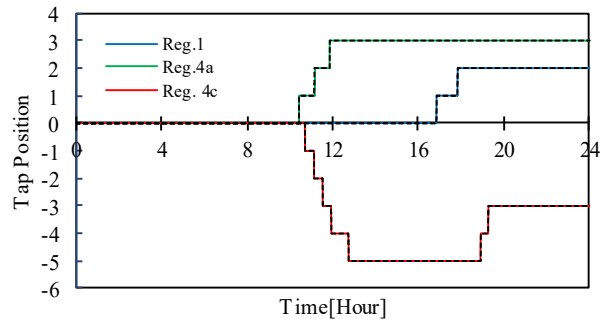


(b) Voltage profiles.

Figure 3.7 Results of Case 0: Without control for the cloudy day.



(a) Voltage profiles.



(b) Tap positions.

Figure 3.8 Results of the proposed controls for the clear day. (Solid lines: case C1 (Optimal); Dashed lines: case C2 (Suboptimal)).

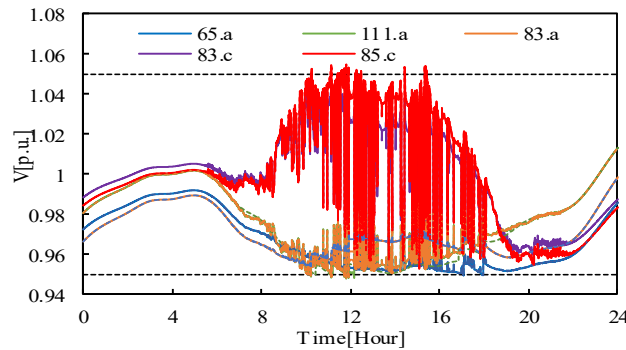
2) Case C1: Proposed method (Optimal)

a) Clear day condition

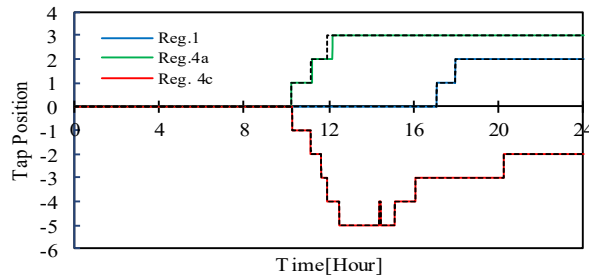
After applying the proposed optimal control strategy, the voltage profiles are improved, where voltage violations are removed as shown in Figure 3.8 (a). Figure 3.8 (b) illustrates the tap position for each regulator; only three regulators act to mitigate the voltage problems. Based on the proposed control strategy at time t , only the regulator with the most effective ability takes action to mitigate the voltage problems. Thus, the proposed method effectively coordinates the tap operations of various voltage regulators, thereby preventing undesirable tap oscillations. The system overall voltage deviation is minimized as illustrated in Table 3.2. Thus, the proposed method can completely solve the voltage violations in the active UDS.

b) Cloudy day condition

A cloudy day of PV generation in Figure 3.5 is used to check the performance of the proposed control strategy in the presence of voltage fluctuations. Applying the proposed control strategy to this case clearly mitigates the voltage violation without tap oscillations, as shown in Figure 3.9 and Table 3.2. The number of tap changes is slightly increased in the cloudy day compared with the clear day because of the PV output



(a) Voltage profiles.



(b) Tap positions.

Figure 3.9 Results of the proposed controls for the cloudy day. (Solid lines: case C1 (Optimal); Dashed lines: case C2 (Suboptimal)).

fluctuations. These results show that the proposed optimal control strategy works effectively to reduce the voltage violations without tap oscillations even in the case of PV output fluctuations.

3) Case C2: Proposed method (Suboptimal)

This case represents the proposed suboptimal method in normal condition. As shown in Figure 3.8, Figure 3.9, and Table 3.2, the performances of the suboptimal method (dashed lines) and the optimal method (solid lines) are almost equivalent. It is noticed from the figures that the regulators react one by one at a different time instant, which implies that the proposed suboptimal law succeeds.

4) Case C3: Proposed method (Suboptimal, Agent failure)

In the case of communication failure among the agents, the performance of the proposed suboptimal method is evaluated. We assume that regulator no. 4 fails to communicate with the BM. The regulator no. 4 agent will act autonomously using only the available data. In this case, since the status of agent no. 4 in the BM has not been updated and is indicated as “0”, the other agents will neglect agent no.4 data and takes their actions to minimize the voltage deviation.

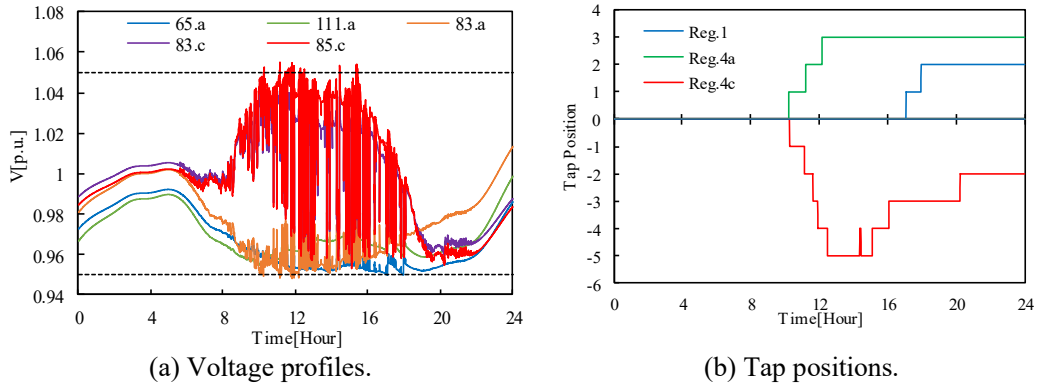
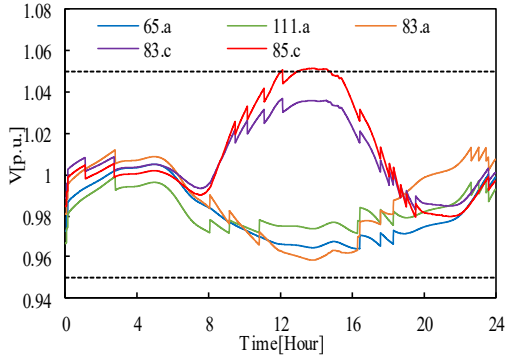


Figure 3.10 Results of case 3: Proposed control for the cloudy day with failure.

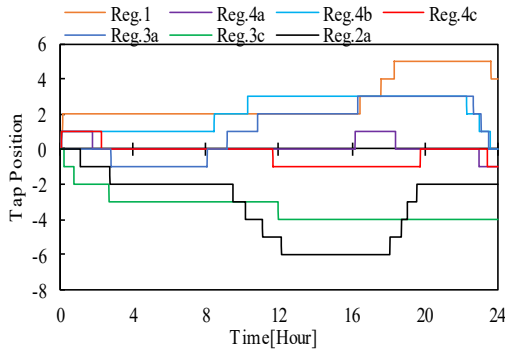
The results for clear and cloudy days are shown in Table 3.2. Both the voltage deviation and number of tap operations are approximately identical to those in the optimal strategy for the clear day. Meanwhile, the voltage deviation is increased for the cloudy day since reg. no.4 works individually based on the suboptimal rule with no cooperation with the other agents as observed in Figure 3.10. Thus, the proposed method works effectively even in the case of communication failure.

Table 3.2 Total voltage deviation and no. of tap changes

Simulation Cases	Clear day		Cloudy day	
	Total VD	Tap changes	Total VD	Tap changes
C0: Without control	33.20	0	23.10	0
C1: Proposed method (Optimal)	0.012	12	0.124	15
C2: Proposed method (Suboptimal.)	0.012	12	0.124	15
C3: Proposed (Suboptimal, agent failure)	0.012	12	0.132	15
C4: Conventional control	0.242	44	0.505	52
C5: Proposed (Optimal, High PV penetration)	0.014	17	0.387	27
C6: Proposed (Suboptimal, High PV penetration)	0.014	17	0.387	27

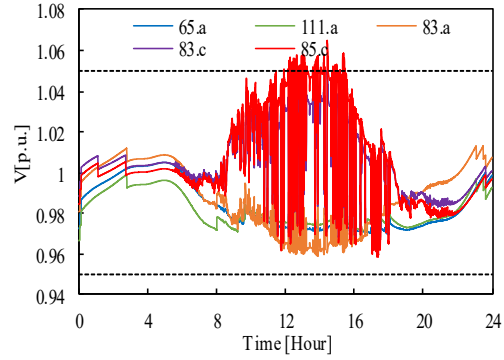


(a) Voltage Profiles

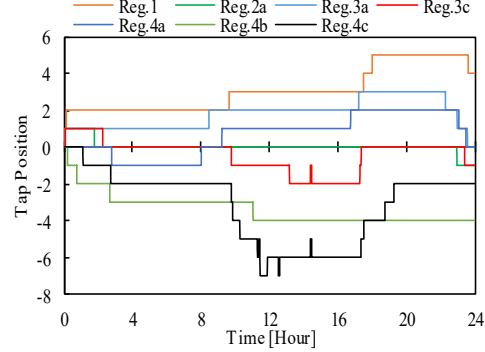


(b) Tap Positions

Figure 3.11 Results of case 4: Conventional control for the clear day.



(a) Voltage Profiles



(b) Tap Positions

Figure 3.12 Results of case 4: Conventional control for the cloudy day.

5) Case C4: Conventional method

Table 3.2 lists the performance of a classical control method, which is the line drop compensator approach in [6], [7]. Figure 3.11 and Figure 3.12 show the voltage profiles and tap operations for clear and cloudy days, respectively. Compared with the conventional method, the proposed method has a high performance in both clear and cloudy days.

6) Cases C5 and C6: Proposed methods (High PV penetration)

In cases C5 and C6, the number of installed PV sources is increased to check the performance of the proposed optimal and suboptimal control strategies, respectively. The

results for the clear and cloudy days are shown in Table 3.2. The observed performances are equivalent in both cases, and the number of tap movement is increased compared with Cases 1 and 2 due to the high PV penetration.

3.6.1.2 Overall Performance Evaluations

Figure 3.13 shows the performance of the proposed optimal and suboptimal control strategies compared with the conventional control method in the case of the clear day. The total voltage deviations vs. number of tap changes are plotted, where parameters α for optimal and α_0 for suboptimal methods are gradually changed from 0 to 1.1×10^{-4} . Each plot is obtained by a 24-hour simulation. The plots of the optimal (circle) and suboptimal (triangle) cases are mostly identical, which implies that the reactions of all regulators (e.g., Figure 3.8 and Figure 3.9) are identical for each 24-hour simulation for different threshold values. Thus, the suboptimal control method can be optimal for a wide range of selected values of α_0 . Figure 3.13 shows that the threshold values α and α_0 are useful to adjust the response time of the controllers. The proposed control system clearly shows a Pareto-optimal characteristic between the number of tap operations and the total voltage deviations.

The performance of the conventional method is also shown in Figure 3.13, where the time delay of the line drop compensators is changed as a parameter. Figure 3.13 also shows the result for the agent failure for the proposed method. The performance of the proposed method degrades in the case of failure, but it remains acceptable, which is better than the conventional method in normal conditions, since the coordination is performed among the normal agents using the available data.

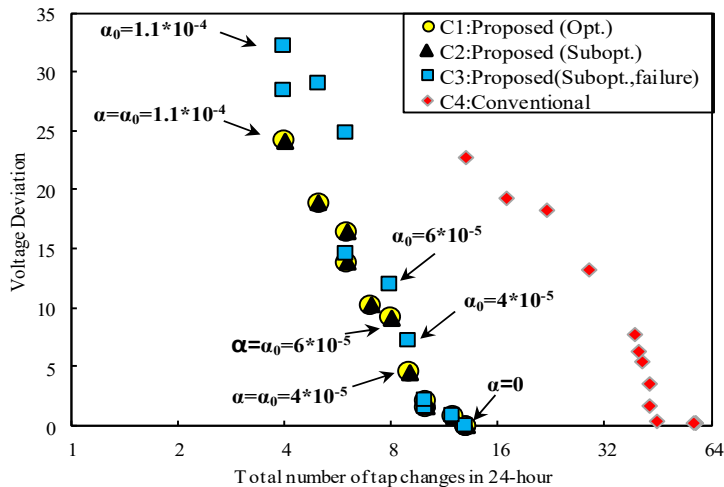


Figure 3.13 Voltage deviation vs. tap change in clear day for different α and α_0 .

3.6.2 IEEE 34-node Test Feeder

The IEEE 34-node test feeder is characterized by the unbalanced loading condition with two three-phase star-connected voltage regulators as shown in Figure 3.14[87]. The proposed control strategy effectively reduces the total voltage deviation with the small number of tap changes compared with the line drop compensator method, as illustrated in the case study of the clear day in Figure 3.15 and Table 3.3.

Table 3.3 also lists the total computation time to determine the control actions for all agents in each control time. The computational burden of the proposed method to obtain the optimal control is sufficiently fast, but it is greater than the conventional method. Thus, the proposed method can effectively act in real-time circumstances.

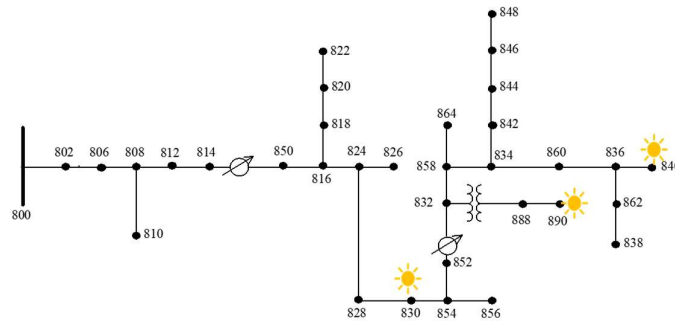


Figure 3.14 IEEE 34-node test feeder.

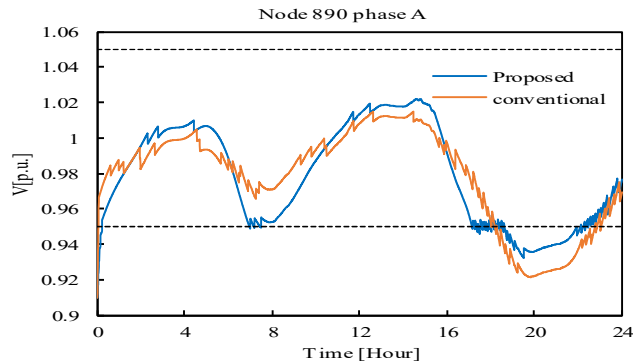


Table 3.3 Results of the IEEE 34-node test feeder.

	Total VD	Tap changes	computation time (sec/step)
Proposed method	3.51	122	0.00210
Conventional control	14.01	165	0.00031

3.7 Conclusions

An effective voltage control strategy is proposed in this paper using an MAS architecture. The objective of the proposed strategy is to optimally minimize the voltage deviation of the UDS under the condition of high PV penetration. The unbalanced features of the DS with different types and configurations of voltage regulators are considered in the formulation. The optimal and suboptimal methods are realized in the proposed voltage control strategy, where each agent can act autonomously based on the available information to minimize the objective. The simulation results show that the proposed strategies can effectively adjust the tap operations to minimize the voltage deviation with no tap oscillations under different sun profiles (sunny or cloudy).

The optimal method requires a comparison process among the indices of the agents, which is more suitable for a centralized control, although it can be applied to an MAS. The suboptimal method avoids the comparison process among the agents, which can be easily realized by a simple decentralized control strategy using the MAS. The proposed suboptimal method shows an equivalent performance to the optimal method and works reliably even in the case of communication failure. The method can be easily applied to the existing voltage regulators within a reasonable cost of investment compared to a centralized scheme.

As part of the future work, we will upgrade the control algorithm to coordinate with the DG reactive power capability and PV smart inverter functionalities. A hierarchical scheme is under development, where each agent in Figure 3.1 will act as a sub-management agent that manages the DGs in its area [72].

Chapter 4: Reactive Power Control of the DGs for Voltage Regulation

4.1 Introduction

This chapter proposes an effective control strategy for voltage regulation in DSs with high DG penetration using the MAS. The proposed strategy is a simple and efficient method for managing the reactive power capability of various types of DG based on voltage/reactive power sensitivity analysis. Comprehensive case studies on IEEE 33 test feeders are carried out to demonstrate the effectiveness of the control strategy. The numerical results show that the proposed strategy can significantly mitigate the overall voltage violation problems in a simple manner.

4.2 Problem Description

This section describes the main objective function of the voltage regulation problem, the proposed control strategy. In addition, it contains the problem formulation and a brief description for the coordination between reactive power control of DGs and traditional voltage regulators.

4.2.1 Objective Function

The main objective function of the voltage regulation strategies is to minimize voltage deviation as follows:

$$\min f(\mathbf{v}) = \sum_{k=1}^N (v_k - v_R)^2 \geq 0, \quad f(v_R) = 0 \quad (4.1)$$

where \mathbf{v} represents a voltage deviation vector at N monitoring nodes, and v_R is reference voltage.

Based on the load flow equations, the voltages in DSs with DGs are a function of the following parameters.

$$\mathbf{v} = h(\mathbf{P}_L, \mathbf{Q}_L, \mathbf{n}, \mathbf{P}_{DG}, \mathbf{Q}_{DG}) \quad (4.2)$$

where:

\mathbf{P}_L , and \mathbf{Q}_L : load parameters (active and reactive power).

\mathbf{n} : Voltage regulator tap positions.

\mathbf{P}_{DG} , and \mathbf{Q}_{DG} : DGs active and reactive power.

4.2.2 Control Strategy of Voltage Regulators

This section describes briefly the optimal voltage regulators control strategy which has been formulated by the authors in [47], [48]. The main objective of this strategy is to find the optimal setting for the voltage regulators tap positions in order to minimize the voltage violation in the DSs with high PV penetration, and the work was extended to consider the unbalanced features of the active DSs as described in the previous chapter [13], [48].

In the control strategy for voltage regulators, it was assumed that, during the control time t , the load parameters and the DG active power did not change substantially, and the DG did not have reactive power capability. So, based on these assumptions, the tap position is the effective parameters which will be optimally controlled to minimize the voltage deviation function (4.1) as described in Chapter 3.

4.2.3 Voltage Control Problem

From the previous studies, we notice that the voltage regulators cannot totally solve the voltage problems in presence of high DG penetration. Therefore, based on (4.2), the reactive power capability of the DGs should be considered with tap control to reduce the stress on the voltage regulators devices.

4.2.4 Time Coordination

The solution for the voltage control problem and the cooperation between DG reactive power and tap operation described in the previous section can be realized using a good time coordination. The effective time coordination strategy between the DG sources and voltage regulators can help a lot to reduce the DSs voltage violation and decrease the stresses on the voltage regulators operation and the DG sources, but the time coordination between the DG reactive power and tap operation will be considered in the future work.

4.3 Reactive Power Control Strategy

4.3.1 Control Strategy

The objective of this strategy is to study the effect of the reactive power capability of DGs on DSs voltage deviation and to find a simple and effective control strategy for DGs reactive power to minimize the overall voltage deviation of the DS. In this strategy, we assumed that during the control period, the load active, reactive power, and the DGs active power will not change substantially. Also, in this study, we will investigate the effect of the DGs reactive power on the voltage deviation with a fixed tap setting.

The change in reactive power at time t will be:

$$Q_{DG}(t+1) = Q_{DG}(t) + \Delta Q_{DG}(t) \quad (4.3)$$

If the reactive power is changed by ΔQ_{DG} , the change in the voltage deviation objective function (4.1) will be:

$$f(v(t+1)) = f(v(t)) + \Delta f(t) \quad (4.4)$$

From (4.4) the change in voltage $\Delta f(t)$ can be described as follows:

$$\begin{aligned} \Delta f(t) &= f(v(t+1)) - f(v(t)) \\ &= \underbrace{\begin{bmatrix} \frac{\partial f}{\partial v} \end{bmatrix}}_{\text{Reactive power index (RPI)}} \cdot \underbrace{\begin{bmatrix} \frac{\partial v}{\partial Q_{DG}} \end{bmatrix}}_{\text{Reactive power index (RPI)}} \cdot \Delta Q_{DG}(t) \\ &= \mathbf{RPI}(t) \cdot \Delta Q_{DG}(t) \end{aligned} \quad (4.5)$$

where,

$\frac{dv}{dQ_{DG}}$: The voltage/reactive power sensitivity matrix calculated from the power flow jacobian.

ΔQ_{DG} : The change in reactive power of DG.

Equation (4.5) can be written as follow:

$$\begin{aligned} \Delta f(t) &= \mathbf{RPI}(t) \cdot \Delta Q_{DG}(t) \\ &= \sum_k^{N_{DG}} RPI_k \cdot \Delta Q_{DGk} \end{aligned} \quad (4.6)$$

where N_{DG} represent the number of the DG sources which have a reactive power capability.

4.3.2 Voltage/Reactive Power Sensitivity Matrix

The voltage/reactive power sensitivity matrix can be calculated from the Jacobian matrix of the power flow as follows:

$$\begin{bmatrix} \Delta \theta \\ \Delta V \end{bmatrix} = \begin{bmatrix} \frac{\partial P}{\partial \theta} & \frac{\partial P}{\partial V} \\ \frac{\partial Q}{\partial \theta} & \frac{\partial Q}{\partial V} \end{bmatrix}^{-1} \cdot \begin{bmatrix} \Delta P \\ \Delta Q \end{bmatrix} = \begin{bmatrix} \frac{\partial \theta}{\partial P} & \frac{\partial \theta}{\partial Q} \\ \frac{\partial V}{\partial P} & \frac{\partial V}{\partial Q} \end{bmatrix} \cdot \begin{bmatrix} \Delta P \\ \Delta Q \end{bmatrix} \quad (4.7)$$

From the previous equations the change in voltage ΔV regarding active and reactive power can be calculated as follows:

$$\begin{aligned}\Delta V &= \frac{\partial V}{\partial P} \cdot \Delta P + \frac{\partial V}{\partial Q} \cdot \Delta Q \\ &= \frac{\partial V}{\partial P} \cdot (\Delta P_L + \Delta P_{DG}) + \frac{\partial V}{\partial Q} \cdot (\Delta Q_L + \Delta Q_{DG})\end{aligned}\quad (4.8)$$

During the control time t , the DG active power will not change substantially. So, the previous equation (4.8) can be rewritten as follows:

$$\begin{aligned}\Delta V &= \frac{\partial V}{\partial Q} \cdot \Delta Q_{DG} \\ \begin{bmatrix} \Delta V_1 \\ \Delta V_2 \\ \vdots \\ \Delta V_{N_{DG}} \end{bmatrix} &= \underbrace{\begin{bmatrix} \frac{\partial V_1}{\partial Q_1} & \dots & \frac{\partial V_1}{\partial Q_{N_{DG}}} \\ \vdots & \ddots & \vdots \\ \frac{\partial V_{N_{DG}}}{\partial Q_1} & \dots & \frac{\partial V_{N_{DG}}}{\partial Q_{N_{DG}}} \end{bmatrix}}_{\text{Voltage/reactive power sensitivity matrix}} \cdot \begin{bmatrix} \Delta Q_{DG_1} \\ \Delta Q_{DG_2} \\ \vdots \\ \Delta Q_{DG_{N_{DG}}} \end{bmatrix}\end{aligned}\quad (4.9)$$

4.3.3 Reactive Power Index (RPI)

Based on (4.5), RPI can be defined as the sensitivity of voltage deviation with respect to the unit change in the controllable reactive power, and it can be written as follows:

$$\mathbf{RPI}(t) = \mathbf{V}d(t) \cdot \frac{dv(t)}{dQ_{DG}(t)} \quad (4.10)$$

In a matrix form,

$$\mathbf{RPI} = \begin{bmatrix} Vd_1 & \dots & Vd_{N_{DG}} \end{bmatrix} \cdot \begin{bmatrix} \frac{\partial V_1}{\partial Q_1} & \dots & \frac{\partial V_1}{\partial Q_{N_{DG}}} \\ \vdots & \ddots & \vdots \\ \frac{\partial V_{N_{DG}}}{\partial Q_1} & \dots & \frac{\partial V_{N_{DG}}}{\partial Q_{N_{DG}}} \end{bmatrix} \quad (4.11)$$

where $Vd_i(t) = v_i(t) - v_R$, represents the voltage deviation at time t for node i with respect to a reference voltage v_R .

From the previous equations, the most important part to find the effective strategy for minimizing and control voltage deviation function in (4.1) is **RPI**, and ΔQ_{DG} as described below.

$$\begin{aligned} \min f(\mathbf{v}(t+1)) &= f(\mathbf{v}(t)) + \min \Delta f(t) \\ &= f(\mathbf{v}(t)) + \min \{RPI(t) \cdot \Delta Q_{DG}(t)\} \end{aligned} \quad (4.12)$$

4.4 Control Process

In the proposed strategy each DG source acts as a control agent, as illustrated in Figure 4.1. The steps for control reactive power of DGs at time instant t are illustrated in the flowchart shown in Figure 4.2 and it can be described as follows:

4.4.1 Monitoring Process

- The load and DGs power are monitored, and the power flow analysis is performed.

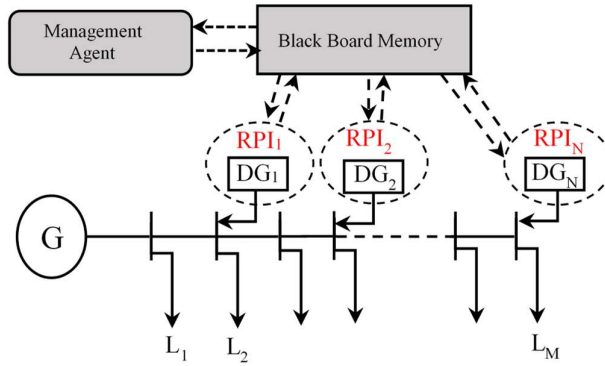


Figure 4.1 Control strategy of DGs reactive power

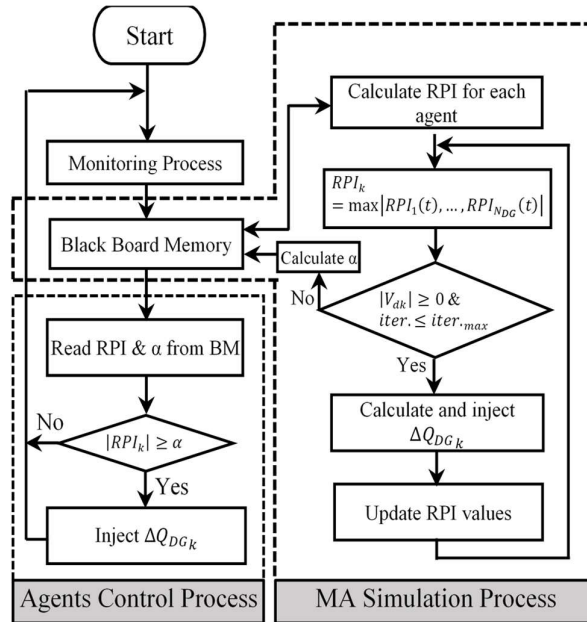


Figure 4.2 Flowchart of the control process.

- Each DG source acts as a control agent, as shown in Figure 4.1..
- Each agent will calculate its voltage deviation and the available amount of reactive power and transfer these values to the black board memory (BM).

4.4.2 Control Process of the Management Agent

When a voltage violation occurs at any time t , the management agent (MA) will be responsible for the following actions in order to minimize $\Delta f(t)$:

- Reads the available information about each agent from the BM.
- Calculates the RPI value for each agent.
- Compares among the values of RPI and determines the agent k which has the highest RPI as described in (4.13).

$$RPI_k(t) = \max \left[RPI_1(t), \dots, RPI_{N_{DG}}(t) \right] \quad (4.13)$$

- Calculates the threshold value α among the agents' RPI , and transfer it with the RPI values to the BM.

4.4.3 Control Process of the Local Agents

- Receives the RPI value and α from the BM.
- If $|RPI| \geq \alpha$, the agent k will inject or absorb a reactive power ΔQ_{DG_k} to minimize the voltage deviation at the local bus subject to:
 - Voltage constrains: $0.95 \leq v_k(t) \leq 1.05$
 - Reactive power constrains:

$$\begin{aligned} -Q_{DG_k}(t) &\leq -\Delta Q_{DG_k}(t) \leq Q_{DG_k}(t) \\ Q_{DG_k}(t) &= \sqrt{S_{DG_k}(t)^2 - P_{DG_k}(t)^2} \end{aligned} \quad (4.14)$$

After injecting or absorbing the calculated ΔQ_{DG_k} by the agent k , the other agents will update its RPI values and the next agent that has the highest value will act. The control process will end when the minimum voltage deviation is achieved, or the maximum reactive power is reached. The control strategy is very effective in simplifying the coordination process among the agents. Also, in case of emergency or lost communication among the agents and the BM, each agent will act independently and achieve the desired goals based on the local data.

4.5 Result and Discussion

4.5.1 Test Feeder

The IEEE 33- distribution test feeder shown in Figure 4.3 is used for simulations and analyses of the proposed control strategy. Three DG sources (PV with inverter) which have reactive power capability, are connected at nodes 10, 14, and 18.

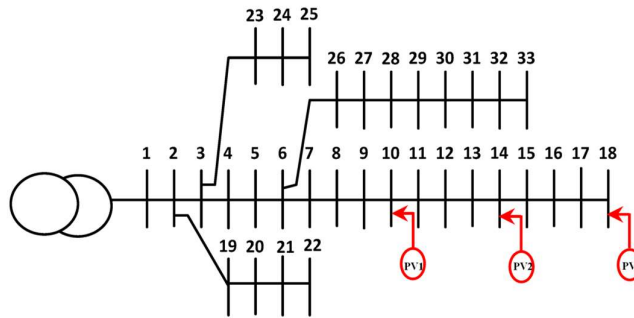


Figure 4.3 IEEE 33-bus test feeder.

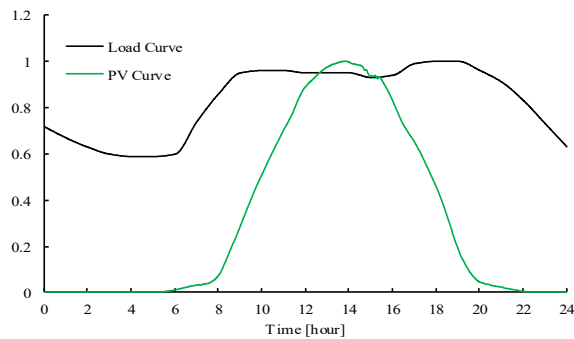


Figure 4.4 Load and PV curves.

4.5.2 Simulated Cases

The proposed control strategy for DGs reactive power has been carried out using MATLAB software with normalized 24-hour load profile and PV curves shown in Figure 4.4. The voltage limits considered in the simulated cases is 1.05 p.u. and 0.95 p.u.

4.5.2.1 Case 1: Low PV Penetration

The rated capacity of each PV source used in this case is 500 kW, and the reactive power supplied by the PV inverter are function of PV active power as described in (4.14).

a) Without reactive power control

Figure 4.5 (a) shows the daily voltage profile for the PV connected nodes. The profile illustrates that the nodes have a voltage drop problems during the PV off-peak time. This demonstrates the important of the reactive power capability of PV in solving voltage violations during night-time in the DSs with low PV penetration.

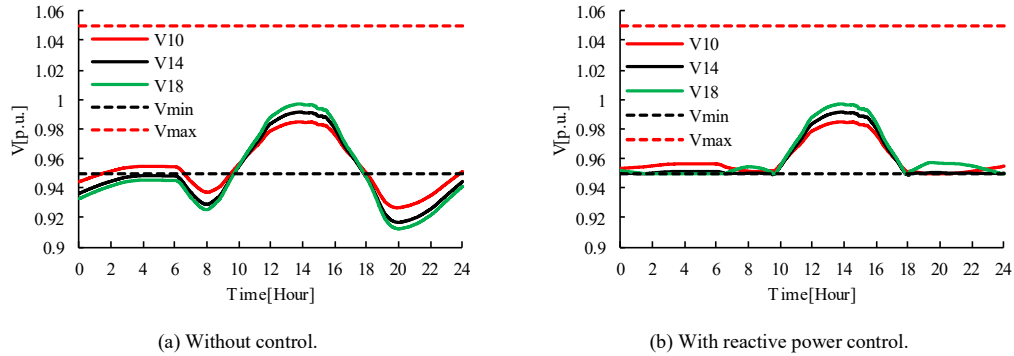


Figure 4.5 Voltage profiles of Case1(Low PV Penetration).

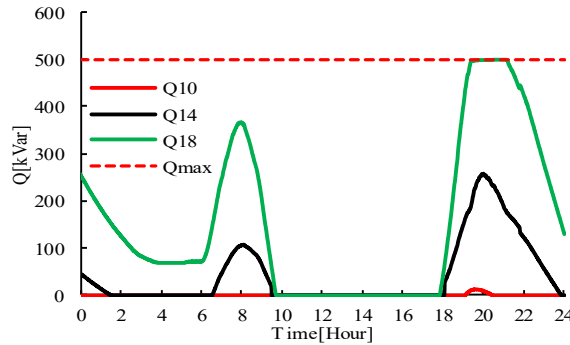


Figure 4.6 Reactive power output of PV sources(Low PV Penetration).

b) With reactive power control

Since, the nodes voltage profiles in Figure 4.5 (a) illustrate that the voltage drop for the three PV nodes occurs simultaneously during most of day time, applying the proposed control strategy will specify the sources from the three PV sources that have the greatest effect on voltage drop mitigation and it should be act first. As shown in Figure 4.5 (b), applying the proposed reactive power control strategy helps to mitigate the voltage drop problems on the three PV nodes.

The reactive power of the PV sources is illustrated in Figure 4.6, demonstrating that the proposed control strategy can effectively manages the reactive power capability of the PV sources. Figure 4.6 shows that reactive power was supplied by the PV sources at node 14 and 18 since it has the highest *RPI* values, and this decreases the amount of reactive power supplied by the other sources. Also, between hours 19:21, the PV at node 18

reaches its maximum reactive power limit, therefore, the next PV source which have the next high *RPI* (PV at nodes 14, and 10) value will act and inject the remaining amount of the required reactive power in order to mitigate the remaining voltage deviation.

4.5.2.2 Case 2: High PV Penetration

In this case, the penetration of the PV sources is increased, to check the performance of the proposed control strategy under such extreme condition. The rated capacity of the three PV sources used in this case is 500, 700, 1400 kW for PV nodes 10, 14, and 18, respectively. Since the reactive power control strategy in this study is simulated at fixed tap position, the reactive power supplied by the PV inverter is increased by increasing the inverter size by 10% to mitigate the voltage problems occurs in the peak time of PV generation.

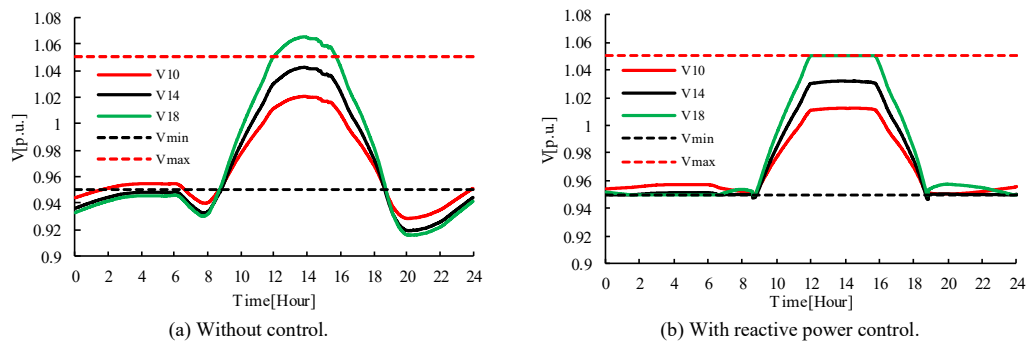


Figure 4.7 Voltage profiles of Case 2(High PV Penetration).

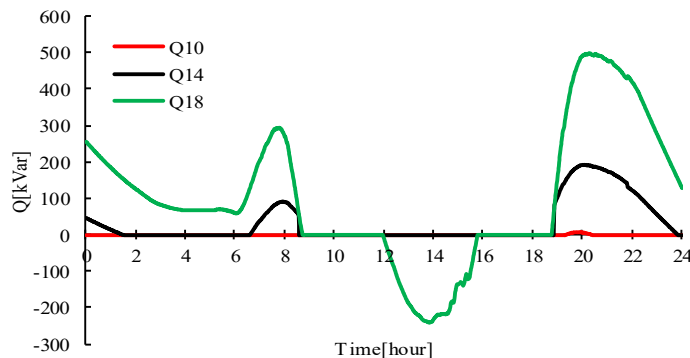


Figure 4.8 Reactive power output of PV sources (High PV penetration).

a) Without reactive power control

Because of high PV penetration, a voltage rise problem occurs at node 18 during the peak time of PV generation as shown in the voltage profiles shown in Figure 4.7 (a). Also, a voltage drop problem still occurs in the PV off-peak time. This indicates that at high PV penetration, both voltage rise, and voltage drop are resulted.

b) With reactive power control

Figure 4.7 (b) illustrates that the proposed control strategy succeeds to solve the voltage rise and the voltage drop problems occur at high PV penetration. And as shown from Figure 4.8 (c), the PV at node 18 injects reactive power during the off-peak generation time to mitigate the voltage drop problem. Increasing the size of the PV inverter by 10% gives the PV at node 18 source the flexibility to mitigate the voltage rise problem occurs at the peak time of PV generation, as illustrated in the reactive power of PV at bus18 (Figure 4.7 (b)).

4.6 Conclusions

This chapter provides a simple and effective control strategy for reactive power of multiple DG sources in the DS. The proposed control strategy is formulated based on the voltage/reactive power sensitivity analysis using MAS architecture, In the proposed strategy, each DG has a reactive power capability is represented as a control agent, and all agents can work together to minimize the overall voltage deviation.

The simulated cases demonstrate that the proposed strategy can mitigate the voltage drop problems and decrease the effect of voltage rise occurred at the peak time of PV generation. Furthermore, the coordination among the PV sources in supplying or absorbing reactive power, decreases the stress on the PV inverters.

Finally, in the proposed strategy each DG has a reactive power capability is represented by a simple index (referred to as *RPI*) and it acts as a control agent, which will help a lot in the coordination process among the DG reactive power and the traditional voltage regulators in the future work.

Chapter 5: Active/Reactive Power Control of DGs Using Nodal Prices

5.1 Introduction

This chapter proposes a novel method for the management of the output power of PV sources in order to realize an optimal operation of DS and solve the voltage raise problem and the unfairness situation in PV generations. The objective of the proposed method is to control the reactive power outputs of PVs to maximize the total output power, while improving the voltage profiles of the DS. In this chapter, two optimization problems are formulated: One is for the optimal operation of DS, where the objective is to maximize the total active power generations of the PVs subject to the voltage limits and PV inverter constraints. The other is for the individual PV prosumers to maximize their profits subject to the inverter constraints. An important thing is that the solutions of the both problems agree to each other by the following procedure:

- (1) The former optimization provides the nodal shadow prices of the active and reactive powers of PV inverter outputs.
- (2) Then prices are announced to the PV prosumers.
- (3) The prosumers maximize their profit under the nodal prices.

The proposed method performs an optimal power flow (OPF) calculation and compute the shadow prices of active and reactive powers based on the multi-agent system approach. Then a dynamic pricing is carried out on-line using LMP for real and reactive powers of PVs in DS. The simulation results confirm that the proposed method can successfully deal with the voltage violations in DS and minimize the curtailment of PV power.

5.2 Proposed Control Strategy

5.2.1 Outline of the Proposed Strategy

The proposed control strategy combines the centralized and the distributed autonomous control as illustrated in Figure 5.1. The information (inverter and PV constraints of local agents, shadow prices from management agent, etc.) is exchanged via a common memory, referred to as blackboard memory (BM) in this paper. Each agent measures local data to send them to BM.

The management agent computes an optimal power flow based on the data from the

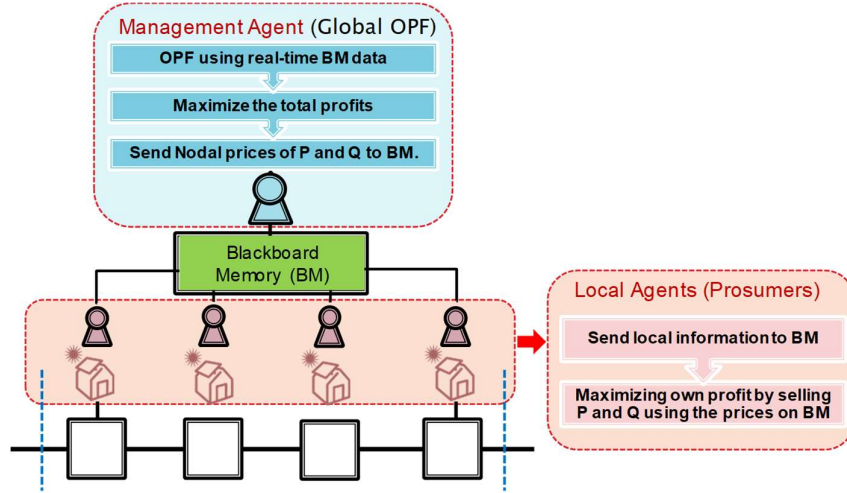


Figure 5.1 Proposed Control System.

agents through BM, and provides active and reactive nodal prices to BM. Then, each agent determines its own behavior and acts independently under the nodal prices provided through BM. Here, the optimal DS operation is realized, while the reactive power of each PV is effectively utilized so that the voltage regulation is performed.

[Management agent]

State estimation of the DS, optimization calculation, and announcement of the nodal prices of active and reactive power.

[PV agent]

Measurement of local data, control of active and reactive powers of PV output.

[Blackboard Memory]

A memory where the management agent and each PV agent share the measured and the calculated data.

5.2.2 Global OPF Formulation for the Management Agent

The objective of global OPF is to maximize the sum of PV generations in DS, equivalent to the total profit, with network constraints and PV inverter constraints as follows:

$$\max_{P_i, Q_i} \sum_{i \in N} F_i(P_i, Q_i) \tag{5.1}$$

Subject to

$$P_i^2 + Q_i^2 \leq S_i^2 \tag{5.2}$$

$$-\gamma_i P_i \leq Q_i \leq \gamma_i P_i \quad (5.3)$$

$$0 \leq P_i \leq \bar{P}_i \quad (5.4)$$

$$V_i \leq V_{\max,i} \quad (5.5)$$

$$\begin{bmatrix} P_i - P_{li} \\ Q_i - Q_{li} \end{bmatrix} = \begin{bmatrix} h_{pi}(\mathbf{V}, \boldsymbol{\delta}) \\ h_{qi}(\mathbf{V}, \boldsymbol{\delta}) \end{bmatrix} \quad (5.6)$$

where,

$i \in N$, $N = \{1, \dots, n\}$, n is the number of PV sources.

$F_i(P_i, Q_i) = w_{pi} P_i$: objective function of PV no. i .

w_{pi} : price of PV active power.

P_i, Q_i : PV active and reactive power.

P_{li}, Q_{li} : active and reactive power of node i .

S_i : capacity of PV inverter.

\bar{P}_i : available active power of PV calculated from solar radiation.

$\gamma_i = \tan \varphi_{\min,i}$, $\varphi_{\min,i}$: lower limit of PV power factor angle.

V_i : voltage at PV connection point i .

$V_{\max,i}$: upper limit of voltage.

δ_i : Phase angle of PV connection point i .

h_{pi}, h_{qi} : power flow equations.

It is assumed that the value of \bar{P}_i is the available value of the PV power output at each node, and it can be determined by the solar radiation. The measurements by radiation meters at representative points are enough for this purpose. In the above calculation process, the state estimation is performed to obtain the parameters of (5.6). This model can use only the voltage and power characteristics of the PV nodes. In this paper, only the upper limit of voltage is considered since voltage raise problem is a main subject of PV output controls.

5.2.3 Formulation of KKT Condition for Global OPF

The optimal solution of (5.1) should satisfy the Karush-Kuhn-Tucker (KKT) condition as follows:

$$L(P, Q, \lambda) = \sum_{i \in N} \left\{ \begin{aligned} &F_i(P_i, Q_i) + \lambda_{1,i}(S_i^2 - P_i^2 - Q_i^2) + \lambda_{2,i}(\gamma_i P_i + Q_i) \\ &+ \lambda_{3,i}(\gamma_i P_i - Q_i) + \lambda_{4,i}P_i + \lambda_{5,i}(\bar{P}_i - P_i) + \lambda_{6,i}(V_{\max,i} - V_i) \\ &+ \mu_{1,i}(h_{p_i}(\mathbf{V}, \boldsymbol{\delta}) - P_i + P_{li}) + \mu_{2,i}(h_{q_i}(\mathbf{V}, \boldsymbol{\delta}) - Q_i + Q_{li}) \end{aligned} \right\} \quad (5.7)$$

$$\frac{\partial L}{\partial P_i} = \frac{\partial F_i}{\partial P_i} - 2\lambda_{1,i}P_i + \lambda_{2,i}\gamma_i + \lambda_{3,i}\gamma_i + \lambda_{4,i} - \lambda_{5,i} - \mu_{1,i} = 0 \quad (5.8)$$

$$\frac{\partial L}{\partial Q_i} = \frac{\partial F_i}{\partial Q_i} - 2\lambda_{1,i}Q_i + \lambda_{2,i} - \lambda_{3,i} - \mu_{2,i} = 0 \quad (5.9)$$

$$\frac{\partial L}{\partial V_i} = -\lambda_{6,i} + \boldsymbol{\mu}_1^T \frac{\partial \mathbf{h}_p}{\partial V_i} + \boldsymbol{\mu}_2^T \frac{\partial \mathbf{h}_q}{\partial V_i} = 0 \quad (5.10)$$

$$\frac{\partial L}{\partial \delta_i} = \boldsymbol{\mu}_1^T \frac{\partial \mathbf{h}_p}{\partial \delta_i} + \boldsymbol{\mu}_2^T \frac{\partial \mathbf{h}_q}{\partial \delta_i} = 0 \quad (5.11)$$

$$\frac{\partial L}{\partial \lambda_{1,i}} = S_i^2 - P_i^2 - Q_i^2 \geq 0, \lambda_{1,i}(S_i^2 - P_i^2 - Q_i^2) = 0 \quad (5.12)$$

$$\frac{\partial L}{\partial \lambda_{2,i}} = \gamma_i P_i + Q_i \geq 0, \lambda_{2,i}(\gamma_i P_i + Q_i) = 0 \quad (5.13)$$

$$\frac{\partial L}{\partial \lambda_{3,i}} = \gamma_i P_i - Q_i \geq 0, \lambda_{3,i}(\gamma_i P_i - Q_i) = 0 \quad (5.14)$$

$$\frac{\partial L}{\partial \lambda_{4,i}} = P_i \geq 0, \lambda_{4,i}P_i = 0 \quad (5.15)$$

$$\frac{\partial L}{\partial \lambda_{5,i}} = \bar{P}_i - P_i \geq 0, \lambda_{5,i}(\bar{P}_i - P_i) = 0 \quad (5.16)$$

$$\frac{\partial L}{\partial \lambda_{6,i}} = V_{\max,i} - V_i \geq 0, \lambda_{6,i}(V_{\max,i} - V_i) = 0 \quad (5.17)$$

$$\frac{\partial L}{\partial \mu_{1,i}} = h_{p_i}(\mathbf{V}, \boldsymbol{\delta}) - P_i + P_{li} = 0 \quad (5.18)$$

$$\frac{\partial L}{\partial \mu_{2,i}} = h_{q_i}(\mathbf{V}, \boldsymbol{\delta}) - Q_i + Q_{li} = 0 \quad (5.19)$$

Here, $\lambda_{1,i}$, $\lambda_{2,i}$, $\lambda_{3,i}$, $\lambda_{4,i}$, $\lambda_{5,i}$, $\lambda_{6,i}$, $\mu_{1,i}$, and $\mu_{2,i}$ are Lagrange multipliers, which are nonnegative. $\boldsymbol{\mu}_1$, $\boldsymbol{\mu}_2$, \mathbf{h}_p , and \mathbf{h}_q are n dimensional vectors. The solution of the above problem provides an optimal power flow. The nodal prices p_{P_i} and p_{Q_i} for active and reactive power outputs, corresponding to the last terms of (5.8) and (5.9), are computed as follows.

$$p_{P_i} = -\mu_{1,i} = -\left(\frac{\partial V}{\partial P_i}\right)^T \boldsymbol{\lambda}_6, p_{Q_i} = -\mu_{2,i} = -\left(\frac{\partial V}{\partial Q_i}\right)^T \boldsymbol{\lambda}_6 \quad (5.20)$$

It is noted that the nodal prices are in general negative for active power and positive for lagging reactive power. The nodal prices will be transferred to the local agents through BM. Then, each agent will maximize its own profit, resulting in the optimal power flow as will be described in the next section.

5.2.4 Profit Maximization for Local Agents

The nodal prices (5.20) are added to the original power prices to form the objective function. Each local agent is to maximize its own Profit f_i as follows:

$$\begin{aligned} \max_{P_i, Q_i} F_i(P_i, Q_i) &= F_i(P_i, Q_i) + p_{P_i} P_i + p_{Q_i} Q_i \\ &= (w_{P_i} + p_{P_i}) P_i + p_{Q_i} Q_i \end{aligned} \quad (5.21)$$

Subject to

$$P_i^2 + Q_i^2 \leq S_i^2 \quad (5.22)$$

$$-\gamma_i P_i \leq Q_i \leq \gamma_i P_i \quad (5.23)$$

$$0 \leq P_i \leq \bar{P}_i \quad (5.24)$$

The KKT conditions are given as follows:

$$L(P_i, Q_i, \lambda_i) = \left\{ \begin{aligned} &F_i(P_i, Q_i) + p_{P_i} P_i + p_{Q_i} Q_i + \lambda_{1,i} (S_i^2 - P_i^2 - Q_i^2) + \lambda_{2,i} (\gamma_i P_i + Q_i) \\ &+ \lambda_{3,i} (\gamma_i P_i - Q_i) + \lambda_{4,i} P_i + \lambda_{5,i} (\bar{P}_i - P_i) \end{aligned} \right\} \quad (5.25)$$

$$\frac{\partial L}{\partial P_i} = \frac{\partial F_i}{\partial P_i} - 2\lambda_{1,i} P_i + \lambda_{2,i} \gamma_i + \lambda_{3,i} \gamma_i + \lambda_{4,i} - \lambda_{5,i} + p_{P_i} = 0 \quad (5.26)$$

$$\frac{\partial L}{\partial Q_i} = \frac{\partial F_i}{\partial Q_i} - 2\lambda_{1,i} Q_i + \lambda_{2,i} - \lambda_{3,i} - p_{Q_i} = 0 \quad (5.27)$$

$$\frac{\partial L}{\partial \lambda_{1,i}} = S_i^2 - P_i^2 - Q_i^2 \geq 0, \quad \lambda_{1,i} (S_i^2 - P_i^2 - Q_i^2) = 0 \quad (5.28)$$

$$\frac{\partial L}{\partial \lambda_{2,i}} = \gamma_i P_i + Q_i \geq 0, \quad \lambda_{2,i} (\gamma_i P_i + Q_i) = 0 \quad (5.29)$$

$$\frac{\partial L}{\partial \lambda_{3,i}} = \gamma_i P_i - Q_i \geq 0, \quad \lambda_{3,i} (\gamma_i P_i - Q_i) = 0 \quad (5.30)$$

$$\frac{\partial L}{\partial \lambda_{4,i}} = P_i \geq 0, \quad \lambda_{4,i} P_i = 0 \quad (5.31)$$

$$\frac{\partial L}{\partial \lambda_{5,i}} = \bar{P}_i - P_i \geq 0, \quad \lambda_{5,i} (\bar{P}_i - P_i) = 0 \quad (5.32)$$

where, $\lambda_{1,i}$, $\lambda_{2,i}$, $\lambda_{3,i}$, $\lambda_{4,i}$, $\lambda_{5,i}$ are Lagrange multipliers, which are nonnegative. The comparison of (5.8) with (5.27), and (5.9) with (5.28), guarantees that the solution of the

global OPF agrees with those of the profit maximizations for local agents when p_{P_i} and p_{Q_i} are set as (5.20). This implies that when each PV agent pursues the maximum profit the voltages of the DS will be automatically controlled, and the total PV power generation will be maximized.

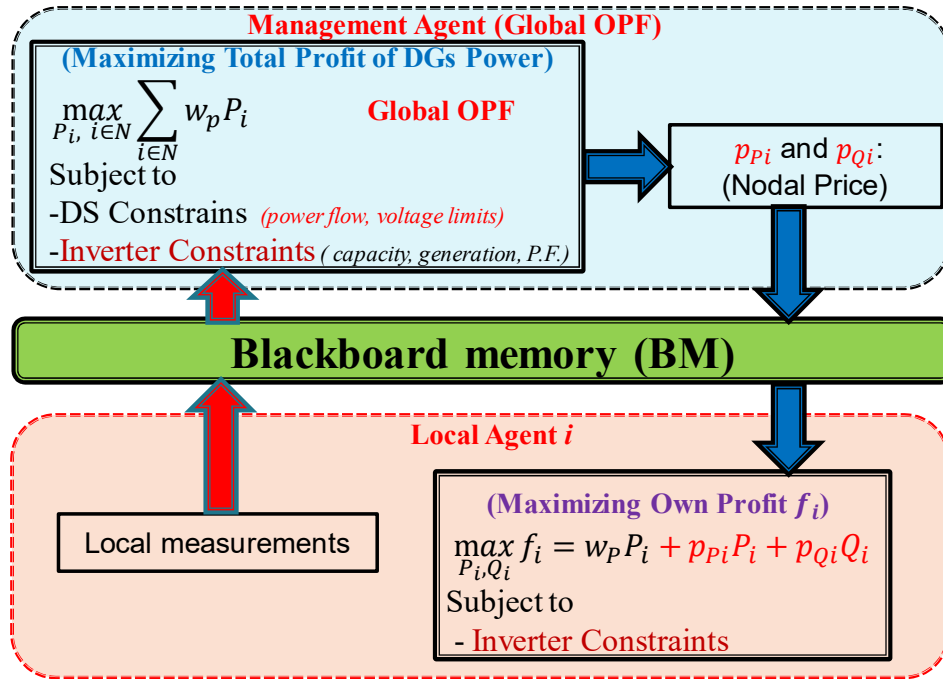


Figure 5.2 The control process of the proposed method.

5.3 Control Process

The control process of the proposed method is shown in Figure 5.2 and it can be described as follows:

5.3.1 Procedure for Management Agent

- [Step M1] Obtain the system parameters, voltage upper limit (V_{max}) and the price of active power (w_p).
- [Step M2] Read parameters of inverters and the local measurements (V, δ, P, Q, \bar{P}) from the agents through BM. Perform state estimation.

[Step M3] Solve the whole system KKT condition to obtain the nodal prices for active power ($w_p + p_p$) and reactive power p_Q , which are transferred to BM.

5.3.2 Procedure for Local Agent i

[step L1] Measure the voltage value (V_i), phase angle (δ_i), active power output (P_i), reactive power output (Q_i), and available active power output (\bar{P}_i).

[step L2] Provide BM with the measurements.

[step L3] Obtain nodal prices ($w_{P_i} + p_{P_i}, p_{Q_i}$) from BM.

[Step L4] Determine the output (P_i and Q_i) to maximize the own profit.

5.4 Simulation Results

5.4.1 Simulation Cases

In order to evaluate the performance of the proposed method, two simulation cases are set as below.

[Case 1] Analysis of a specific operating point.

[Case 2] 24-hour simulation.

In the simulation cases, a system with four connected PV sources is used as shown in Figure 5.3. System parameters are given in Appendix A. Parameters set in the simulation are: $w_{P_i} = 22.68$ [¥ / kWh], $V_{max,i} = 1.02$ [p. u.], $\gamma_i = 0.6197$ corresponding to power factor lower limit, $\cos\phi_{min,i} = 0.85$. The proposed method is compared with a typical conventional control method being used in Japan [88]. The conventional method is a local control to maximize the own active power generation under the above voltage and power factor limits, which is described in Appendix C.

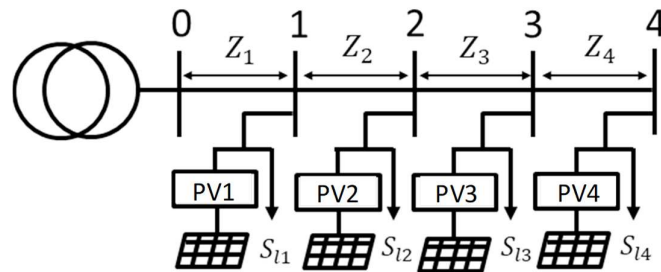


Figure 5.3 5-bus test feeder.

5.4.1.1 Case1: Analysis of A specific Operating Point

Table 5.1 Comparison of the conventional and the proposed method (Case 1)

	Conventional Method					Proposed Method				
	V [p. u.]	P [kWh]	Q [kVArh]	Curtailed P [kWh]	Profits [¥/h] [%]	V [p. u.]	P [kWh]	Q [kVArh]	Curtailed P [kWh]	Profits [¥/h] [%]
PV1	1.010	120.0	0	0	2268 (29)	1.009	119.5	11.1	0.5	2082 (27)
PV2	1.017	120.0	0	0	2268 (29)	1.015	117.6	24.1	2.4	1934 (26)
PV3	1.020	116.8	27.4	3.2	2195 (28)	1.019	113.6	38.6	6.4	1824 (24)
PV4	1.020	65.4	40.6	54.6	1030 (14)	1.020	107.1	54.0	12.9	1754 (23)
Total		422.2	68.0	57.8	7761 (100)		457.8	127.8	22.2	7594 (100)

In this section, the performance of the proposed control method is examined at a fixed operating point, where the available PV active power at each node is 120 [kW] (0.04 [p. u.]) The outputs of the PVs for the conventional and the proposed control methods are listed in Table 5.1, where P , Q and V are the active power, reactive power outputs and the node voltages, respectively. The amount of curtailed active power is calculated from the available power as $120-P$.

Table 5.2 Prices of P and Q offered by the management agent

	Conventional Method		Proposed Method	
	P [¥/kWh]	Q [¥/kVArh]	P [¥/kWh]	Q [¥/kVArh]
PV1	22.68	0	20.82	1.93
PV2	22.68	0	19.03	3.90
PV3	22.68	0	17.27	5.86
PV4	22.68	0	15.47	7.80

It is observed from Table 5.1 that the total amount of power generation is increased, and the curtailed power is significantly decreased compared with those of the conventional method. This implies that the proposed method successfully maximizes the total power generation while controlling the voltages within their limits. The profit per hour for each agent is also given in Table 5.1, which is calculated using the nodal prices for active and reactive powers shown in Table 5.2. As is noticed from the profits, an unfairness situation occurs in the conventional control method. This situation comes from a general tendency that the largest amount of curtailed power is occurred at the end of the feeder. On the other hand, the proposed method realizes a fair profit situation

5.4.1.2 Case2: 24-hour Simulation

In this section, the performance of the proposed method is evaluated using a real fluctuated PV data and load consumptions for nodes 1 to 4 shown in Figure 5.4. The simulation is performed for 24-hour with a time interval of 1 minute.

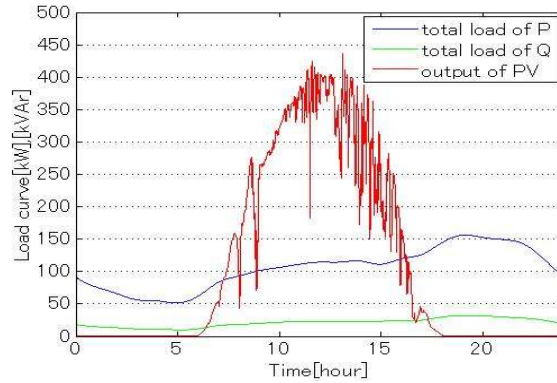


Figure 5.4 Real load and PV output pattern for simulation.

Table 5.3 lists the PV power outputs, the curtailed active power, and the profits for the proposed method and the conventional method. In the proposed method, the total power generation is increased, and the total amount of curtailed power is significantly decreased compared with those of the conventional method. Furthermore, the profits are fairly

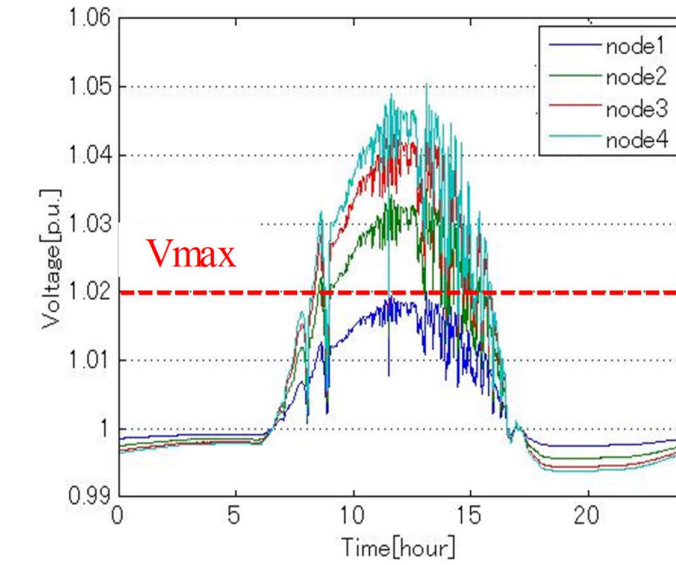
Table 5.3 Generated powers and profits for 24-hour simulation (Case 2)

	Conventional Method				Proposed Method			
	<i>P</i> [kWh]	<i>Q</i> [kVArh]	Curtailed <i>P</i> [kWh]	Profits [%]	<i>P</i> [kWh]	<i>Q</i> [kVArh]	Curtailed <i>P</i> [kWh]	Profits [%]
PV1	866.4	0	0	29	862.8	65.83	3.61	27
PV2	866.4	0	0	29	849.2	147.8	17.2	26
PV3	831.9	177.8	34.5	28	821.4	238.9	45.0	24
PV4	455.6	178.3	410.8	14	784.2	322.2	82.2	23
Total	3020.3	356.1	445.3	100	3317.6	774.7	148	100

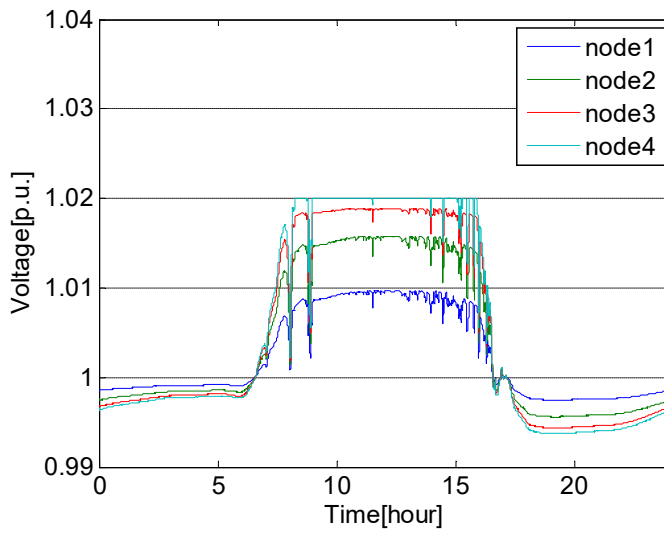
distributed among the agents which implies that the proposed method is also effective from the economic point of view.

Figure 5.5 illustrates the voltage profiles before and after applying the proposed method. It is observed that the method succeeds in controlling the voltages within limits. Figure 5.6 shows the active power output, reactive power output, power factor, and the voltage profiles for the conventional and the proposed control methods. It is noticed from the figures that the proposed method determines the appropriate output of the PV nodes

which realize the fair operation and maximize the power generation for the 24-hour operation.

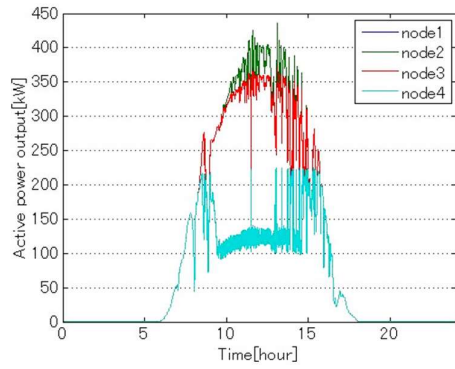


(a) Without control.

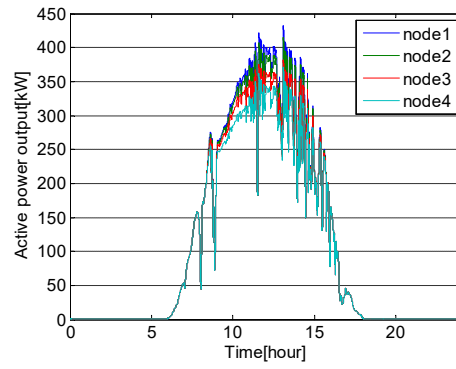


(b) Proposed control method.

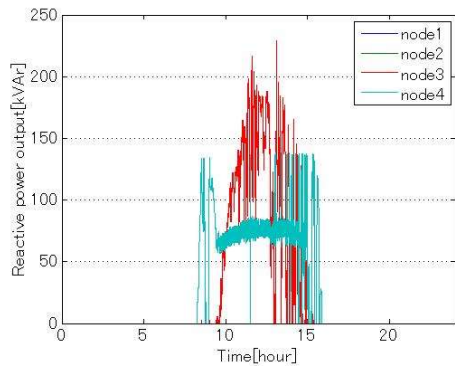
Figure 5.5 Voltage profiles.



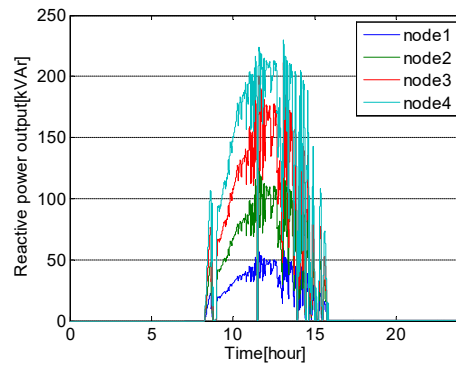
Active power output



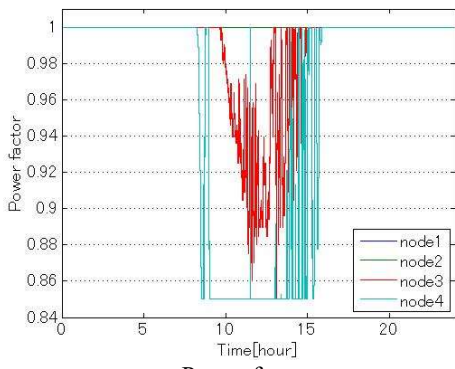
Active power output



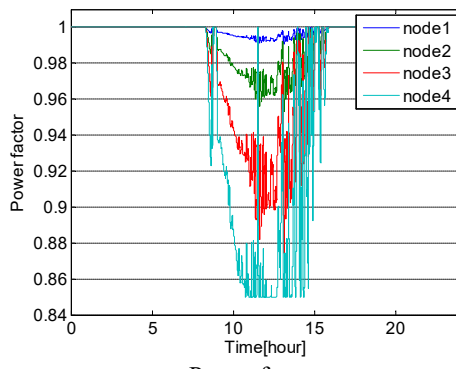
Reactive power output.



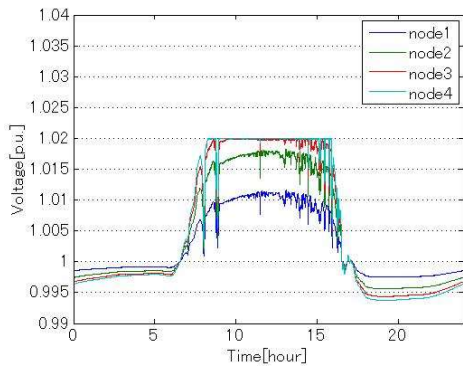
Reactive power output.



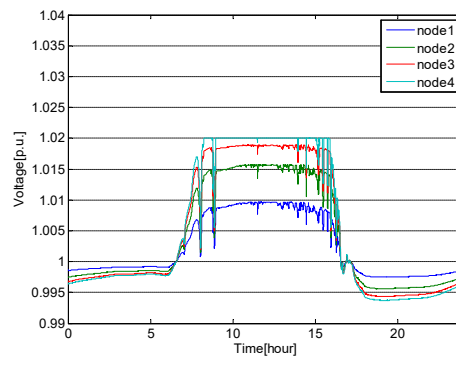
Power factor.



Power factor.



Voltage profile.



Voltage profile.

(a) Conventional Method.

(b) Proposed method.

Figure 5.6 Conventional method vs. proposed method.

5.4.2 Effect of Control Cycle on the Control Performance

In the proposed method, the data of the local agents and the management agent are exchanged asynchronously through the BM. Each agent decides its own action independently based on the nodal prices which are provided by the management agent. Therefore, the control cycle of calculating the nodal prices and the agent control action affects the performance of the proposed method. Figure 5.7 shows that the voltage violation (RMS value) is decreased for higher speed control cycle.

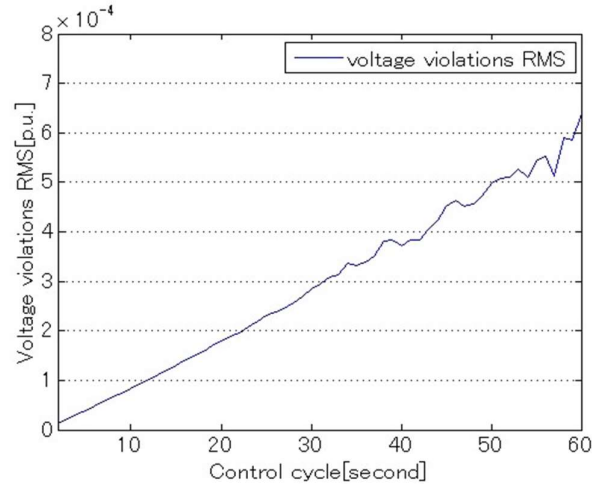


Figure 5.7 Total voltage violations vs. control cycle for 24-hours (RMS p.u).

5.5 Conclusions

In this chapter, a novel voltage control strategy is proposed for the management of the PVs output powers in the DS based on the MAS architecture. The objective of the proposed method is to maximize the total active power generation of the PVs by controlling their active and reactive power outputs using their nodal prices, while maintaining the voltage within normal limits and realizing the optimal operation of the DS.

The simulation results confirm that the proposed method can reduce the total amount of curtailed power produced by the PVs. Furthermore, the profits of the PV agents are fairly distributed among them, which may be able to solve unfairness problem underlying in the existing system. The proposed method achieves the optimal operation of the DS in a distributed manner based on an acceptably simple communication system.

Chapter 6: Conclusions and Future works

The installation of DGs in DSs greatly impacts the performance and reliability of the network and increase the voltage violations. The dissertation focuses on the voltage control schemes. In the following section, the contributions of this dissertation to the voltage control in the DS are highlighted, followed by a list of possible works for future research that have been detected during this research.

6.1 Novelty and Conclusions of the Dissertation

The most important new scientific results of the present dissertation can be summarized as follows:

Optimal control strategy for voltage regulators

An effective and optimal control strategy for voltage regulators is proposed in this thesis using the MAS architecture. The objective of the proposed strategy is to optimally minimize the voltage deviation of the UDS under the condition of high PV penetration. The unbalanced features of the DS with different types and configurations of voltage regulators are considered in the formulation. The optimal and suboptimal methods are realized in the proposed voltage control strategy, where each agent can act autonomously based on the available information to minimize the objective. The simulation results show that the proposed strategies can effectively adjust the tap operations to minimize the voltage deviation with no tap oscillations under different sun profiles.

The optimal method requires a comparison process among the indices of the agents, which is more suitable for a centralized control, although it can be applied to an MAS. The suboptimal method avoids the comparison process among the agents, which can be easily realized by a simple decentralized control strategy using the MAS. The proposed suboptimal method shows an equivalent performance to the optimal method and works reliably even in the case of communication failure. The method can be easily applied to the existing voltage regulators within a reasonable cost of investment compared to a centralized scheme.

Control of the DGs power

Two strategies for voltage control are proposed in the thesis by controlling the DGs powers. Firstly, a simple and effective strategy for reactive power control of the DG sources in the DSs. The proposed control strategy is formulated based on voltage/reactive

power sensitivity analysis using the MAS architecture, In the proposed strategy, each DG with its reactive power capability acts as a control agent, and all agents work together to achieve the minimum voltage deviation. The simulated cases for controlling the PV reactive power, demonstrated that the proposed strategy can mitigate the voltage violations and decrease the stress on the PV inverters.

Secondly, A novel strategy is proposed for the management of the DGs output powers in the DS using nodal prices and MAS architecture. The objective of the proposed method is to maximize the total active power generation of the PVs by controlling their active and reactive power outputs using nodal prices, while maintaining the voltage within normal limits and realizing the optimal operation of the DS. The simulation results confirm that the proposed method can reduce the total amount of curtailed power produced by the PVs. Furthermore, the profits of the PV agents are fairly distributed among them, which may be able to solve unfairness problem underlying in the existing system. The proposed method achieves the optimal operation of the DS in a distributed manner based on an acceptably simple communication system.

6.2 Future Works

There are several research points and interesting topics around the topic of voltage control in active DS have been revealed and need more investigations. Emerging research problems that come from this research include the following:

- Modeling and study different types of the DGs such as wind turbines, fuel cell and diesel generations system.
- Upgrade the proposed control algorithm of the voltage regulators to coordinate with the control schemes of DGs power and PV smart inverter functionalities.
- Upgrading the MAS to operate in the Microgrid concept.
- Further work on the implementation of the MAS is needed. The hardware requirements for fast and reliable operation need to be studied. An appropriate means of communication needs to be addressed.
- Develop a hierarchical scheme, where each agent acts as a sub-management agent that manages the DGs and control the voltages in its area.

References

- [1] REN 21 Renewables Now, “Renewables Global Status Report 2019,” 2019.
- [2] R. A. Walling, R. Saint, R. C. Dugan, J. Burke, and L. A. Kojovic, “Summary of Distributed Resources Impact on Power Delivery Systems,” *IEEE Trans. Power Deliv.*, vol. 23, no. 3, pp. 1636–1644, Jul. 2008.
- [3] N. Mahmud and A. Zahedi, “Review of control strategies for voltage regulation of the smart distribution network with high penetration of renewable distributed generation,” *Renew. Sustain. Energy Rev.*, vol. 64, no. March, pp. 582–595, 2016.
- [4] D. Santos-Martin, S. Lemon, J. D. Watson, A. R. Wood, A. J. V. Miller, and N. R. Watson, “Impact of solar photovoltaics on the low-voltage distribution network in New Zealand,” *IET Gener. Transm. Distrib.*, vol. 10, no. 1, pp. 1–9, 2016.
- [5] R. Tonkoski, D. Turcotte, and T. H. M. El-Fouly, “Impact of high PV penetration on voltage profiles in residential neighborhoods,” *IEEE Trans. Sustain. Energy*, vol. 3, no. 3, pp. 518–527, 2012.
- [6] W. H. Kersting, “Distribution feeder voltage regulation control,” *IEEE Trans. Ind. Appl.*, vol. 46, no. 2, pp. 620–626, May 2010.
- [7] W. H. Kersting, *Distribution system modelling and analysis*. 2002.
- [8] B. A. Robbins, S. Member, and A. D. Domínguez-garcía, “Optimal Reactive Power Dispatch for Voltage Regulation in Unbalanced Distribution Systems,” pp. 1–11, 2016.
- [9] J. R. Castro, M. Saad, S. Lefebvre, D. Asber, and L. Lenoir, “Optimal voltage control in distribution network in the presence of DGs,” *Int. J. Electr. Power Energy Syst.*, vol. 78, pp. 239–247, 2016.
- [10] T. S. Vitor, S. Member, and J. C. M. Vieira, “Optimal Voltage Regulation in Distribution Systems With Unbalanced Loads and Distributed Generation,” 2016, pp. 1–6.
- [11] Z. G.; D. T. Rzy, “Neural Network For Combined Control of Capacitor Banks and Voltage Regulators in Distribution System 00544277.pdf.”
- [12] Yuan-Yih Hsu and Feng-Chang Lu, “A combined artificial neural network-fuzzy dynamic programming approach to reactive power/voltage control in a distribution substation,” *IEEE Trans. Power Syst.*, vol. 13, no. 4, pp. 1265–1271, 1998.
- [13] A. Bedawy, N. Yorino, and K. Mahmoud, “Optimal decentralized voltage control in unbalanced distribution networks with high PV penetration,” in *2017 Nineteenth International Middle East Power Systems Conference (MEPCON)*, 2017, pp. 1373–1377.
- [14] A. Elmitwally, M. Elsaid, M. Elgamal, and Z. Chen, “A Fuzzy-Multiagent Self-Healing Scheme for a Distribution System with Distributed Generations,” *IEEE Trans. Power Syst.*, vol. 30, no. 5, pp. 2612–2622, 2015.
- [15] Y. Zoka *et al.*, “An effective method for distributed voltage control on system reconfiguration and improper motion of voltage control devices for distribution networks,” *IEEJ Trans. Power Energy*, vol. 138, no. 1, pp. 14–22, 2018.
- [16] H. E. Z. Farag and E. F. El-Saadany, “A novel cooperative protocol for distributed voltage control in active distribution systems,” *IEEE Trans. Power Syst.*, vol. 28, no. 4, pp. 1645–1656, 2013.
- [17] F. Ren, M. Zhang, and D. Sutanto, “A multi-agent solution to distribution system management by considering distributed generators,” *IEEE Trans. Power Syst.*, vol. 28, no. 2, pp. 1442–1451, 2013.
- [18] Y. Kim, S. Ahn, P. Hwang, and S. Member, “Coordinated Control of a DG and Voltage

- Control Devices Using a Dynamic Programming Algorithm,” vol. 28, no. 1, pp. 42–51, 2013.
- [19] A. Majumdar, Y. P. Agalgaonkar, B. C. Pal, and R. Gottschalg, “Centralized Volt–Var Optimization Strategy Considering Malicious Attack on Distributed Energy Resources Control,” *IEEE Trans. Sustain. Energy*, vol. 9, no. 1, pp. 148–156, Jan. 2018.
- [20] S. Deshmukh, B. Natarajan, and A. Pahwa, “Voltage/VAR control in distribution networks via reactive power injection through distributed generators,” *IEEE Trans. Smart Grid*, vol. 3, no. 3, pp. 1226–1234, 2012.
- [21] A. Abessi, V. Vahidinasab, and M. S. Ghazizadeh, “Centralized support distributed voltage control by using end-users as reactive power support,” *IEEE Trans. Smart Grid*, vol. 7, no. 1, pp. 178–188, Jan. 2016.
- [22] H. S. Bidgoli and T. Van Cutsem, “Combined Local and Centralized Voltage Control in Active Distribution Networks,” *IEEE Trans. Power Syst.*, vol. 33, no. 2, pp. 1374–1384, 2018.
- [23] L. Wang, D. H. Liang, A. F. Crossland, P. C. Taylor, D. Jones, and N. S. Wade, “Coordination of Multiple Energy Storage Units in a Low-Voltage Distribution Network,” *IEEE Trans. Smart Grid*, vol. 6, no. 6, pp. 2906–2918, Nov. 2015.
- [24] S. Gupta, V. Kekatos, and W. Saad, “Optimal Real-Time Coordination of Energy Storage Units as a Voltage-Constrained Game,” *IEEE Trans. Smart Grid*, pp. 1–1, 2018.
- [25] J. Krata and T. K. Saha, “Real-Time Coordinated Voltage Support with Battery Energy Storage in a Distribution Grid Equipped with Medium-Scale PV Generation,” *IEEE Trans. Smart Grid*, vol. 10, no. 3, pp. 3486–3497, 2019.
- [26] L. Wang, F. Bai, R. Yan, and T. K. Saha, “Real-Time Coordinated Voltage Control of PV Inverters and Energy Storage for Weak Networks with High PV Penetration,” *IEEE Trans. Power Syst.*, vol. 33, no. 3, pp. 3383–3395, May 2018.
- [27] H. Zhao, M. Hong, W. Lin, and K. A. Loparo, “Voltage and Frequency Regulation of Microgrid With Battery Energy Storage Systems,” *IEEE Trans. Smart Grid*, pp. 1–1, 2017.
- [28] X. Yang, Y. Du, J. Su, L. Chang, Y. Shi, and J. Lai, “An Optimal Secondary Voltage Control Strategy for an Islanded Multibus Microgrid,” *IEEE J. Emerg. Sel. Top. Power Electron.*, vol. 4, no. 4, pp. 1236–1246, Dec. 2016.
- [29] T. Ding, C. Li, Y. Yang, J. Jiang, Z. Bie, and F. Blaabjerg, “A Two-Stage Robust Optimization for Centralized-Optimal Dispatch of Photovoltaic Inverters in Active Distribution Networks,” *IEEE Trans. Sustain. Energy*, vol. 8, no. 2, pp. 744–754, Apr. 2017.
- [30] C. Wu, G. Hug, and S. Kar, “Smart inverter for voltage regulation: Physical and market implementation,” *IEEE Trans. Power Syst.*, vol. 33, no. 6, pp. 6181–6192, 2018.
- [31] M. H. Cintuglu, T. Youssef, and O. A. Mohammed, “Development and Application of a Real-Time Testbed for Multiagent System Interoperability: A Case Study on Hierarchical Microgrid Control,” *IEEE Trans. Smart Grid*, vol. PP, no. 99, pp. 1–1, 2016.
- [32] M. Zeraati, M. E. Hamedani Golshan, and J. Guerrero, “Distributed Control of Battery Energy Storage Systems for Voltage Regulation in Distribution Networks with High PV Penetration,” *IEEE Trans. Smart Grid*, vol. 3053, no. c, pp. 1–1, 2016.
- [33] P. M. S. Carvalho, P. F. Correia, and L. a F. Ferreira, “Distributed Reactive Power Generation Control for Voltage Rise Mitigation in Distribution Networks,” *IEEE Trans. Power Syst.*, vol. 23, no. 2, pp. 766–772, 2008.
- [34] P. Jahangiri and D. C. Aliprantis, “Distributed Volt/VAr control by PV inverters,” *IEEE*

- Trans. Power Syst.*, vol. 28, no. 3, pp. 3429–3439, 2013.
- [35] G. Cavraro and R. Carli, “Local and Distributed Voltage Control Algorithms in Distribution Networks,” *IEEE Trans. Power Syst.*, vol. 33, no. 2, pp. 1420–1430, Mar. 2018.
- [36] M. Chamana, B. H. Chowdhury, and F. Jahanbakhsh, “Distributed Control of Voltage Regulating Devices in the Presence of High PV Penetration to Mitigate Ramp-Rate Issues,” *IEEE Trans. Smart Grid*, vol. 9, no. 2, pp. 1086–1095, Mar. 2018.
- [37] E. Dall’anese, H. Zhu, and G. B. Giannakis, “Distributed Optimal Power Flow for Smart Microgrids,” *IEEE Trans. Smart Grid*, vol. 4, no. 3, 2013.
- [38] S. Bolognani, R. Carli, G. Cavraro, and S. Zampieri, “Distributed Reactive Power Feedback Control for Voltage Regulation and Loss Minimization,” *IEEE Trans. Automat. Contr.*, vol. 60, no. 4, pp. 966–981, 2015.
- [39] B. Zhang, A. Y. S. Lam, A. D. Dominguez-Garcia, and D. Tse, “An Optimal and Distributed Method for Voltage Regulation in Power Distribution Systems,” *IEEE Trans. Power Syst.*, vol. 30, no. 4, pp. 1714–1726, Jul. 2015.
- [40] Y. Yang, H. Li, A. Aichhorn, J. Zheng, and M. Greenleaf, “Sizing strategy of distributed battery storage system with high penetration of photovoltaic for voltage regulation and peak load shaving,” *IEEE Trans. Smart Grid*, vol. 5, no. 2, pp. 982–991, 2014.
- [41] M. Castilla, M. Velasco, J. Miret, P. Martí, and A. Momeneh, “Comparative study of reactive power control methods for photovoltaic inverters in low-voltage grids,” *IET Renew. Power Gener.*, vol. 10, no. 3, pp. 310–318, 2016.
- [42] E. Demirok, P. C. González, K. H. B. Frederiksen, D. Sera, P. Rodriguez, and R. Teodorescu, “Local reactive power control methods for overvoltage prevention of distributed solar inverters in low-voltage grids,” *IEEE J. Photovoltaics*, vol. 1, no. 2, pp. 174–182, 2011.
- [43] M. a. Mahmud, M. J. Hossain, H. R. Pota, and a. B. M. Nasiruzzaman, “Voltage control of distribution networks with distributed generation using reactive power compensation,” *IECON 2011 - 37th Annu. Conf. IEEE Ind. Electron. Soc.*, pp. 985–990, 2011.
- [44] X. Liu, A. M. Cramer, and Y. Liao, “Reactive power control methods for photovoltaic inverters to mitigate short-term voltage magnitude fluctuations,” *Electr. Power Syst. Res.*, vol. 127, pp. 213–220, Oct. 2015.
- [45] M. Glavic, “Agents and Multi-Agent Systems: A Short Introduction for Power Engineers,” Liege, BELGIUM, 2006.
- [46] S. D. J. McArthur *et al.*, “Multi-Agent Systems for Power Engineering Applications—Part 1: Concepts, Approaches, and Technical Challenges,” *IEEE Trans. Power Syst.*, vol. 22, no. 4, pp. 1743–1752, 2007.
- [47] N. Yorino, Y. Zoka, M. Watanabe, and T. Kurushima, “An Optimal Autonomous Decentralized Control Method for Voltage Control Devices by Using a Multi-Agent System,” *IEEE Trans. Power Syst.*, vol. 30, no. 5, pp. 2225–2233, Sep. 2015.
- [48] A. Bedawy, N. Yorino, K. Mahmoud, Y. Zoka, and Y. Sasaki, “Optimal Voltage Control Strategy for Voltage Regulators in Active Unbalanced Distribution Systems Using Multi-Agents,” *IEEE Trans. Power Syst.*, pp. 1–1, Sep. 2019.
- [49] N. Yorino, T. Watakabe, Y. Nakamura, Y. Sasaki, Y. Zoka, and A. B. K. Hussien, “A novel voltage control method for distribution systems based on P&Q nodal prices for distributed generations,” *IEEJ Trans. Power Energy*, vol. 139, no. 3, pp. 178–185, 2019.
- [50] R. Tonkoski, L. A. C. Lopes, and T. H. M. El-Fouly, “Coordinated active power curtailment of grid connected PV inverters for overvoltage prevention,” *IEEE Trans.*

- Sustain. Energy*, vol. 2, no. 2, pp. 139–147, Apr. 2011.
- [51] Y. Fan, B. Zhao, Q. Jiang, and Y. Cao, “Peak capacity calculation of distributed photovoltaic source with constraint of over-voltage,” *Autom. Electr. Power Syst.*, vol. 36, pp. 40–44, Sep. 2012.
- [52] R. Comfort, M. Gonzalez, A. Mansoor, P. Barker, P. Short, and A. Sundaram, “Power quality impact of distributed generation : effect on steady state voltage regulation,” *Jakość i Użytkowanie Energii Elektr.*, vol. T. 7, z. 2, pp. 35–42, 2001.
- [53] I. Voloh, T. Ernst -Ge, and G. Solutions, “Review of Capacitor Bank Control Practices.”
- [54] D. Mondal, A. Chakrabarti, and A. Sengupta, “Models of Power Network and Relevant Power Equipments,” in *Power System Small Signal Stability Analysis and Control*, Elsevier, 2014, pp. 41–84.
- [55] C. K. Das, O. Bass, G. Kothapalli, T. S. Mahmoud, and D. Habibi, “Overview of energy storage systems in distribution networks: Placement, sizing, operation, and power quality,” *Renewable and Sustainable Energy Reviews*, vol. 91. Elsevier Ltd, pp. 1205–1230, 01-Aug-2018.
- [56] T. Xu and P. C. Taylor, “Voltage Control Techniques for Electrical Distribution Networks Including Distributed Generation,” *IFAC Proc. Vol.*, vol. 41, no. 2, pp. 11967–11971, 2008.
- [57] X. Liu, A. Aichhorn, L. Liu, and H. Li, “Coordinated control of distributed energy storage system with tap changer transformers for voltage rise mitigation under high photovoltaic penetration,” *IEEE Trans. Smart Grid*, vol. 3, no. 2, pp. 897–906, 2012.
- [58] Y. Wang, K. T. Tan, X. Y. Peng, and P. L. So, “Coordinated Control of Distributed Energy-Storage Systems for Voltage Regulation in Distribution Networks,” *IEEE Trans. Power Deliv.*, vol. 31, no. 3, pp. 1132–1141, 2016.
- [59] Y. Liu, S. Member, J. Li, L. Wu, and S. Member, “Coordinated Optimal Network Reconfiguration and Voltage Regulator / DER Control for Unbalanced Distribution Systems,” vol. 3053, no. c, pp. 1–10, 2018.
- [60] F. Ding and K. A. Loparo, “Hierarchical decentralized network reconfiguration for smart distribution systems - Part I: Problem formulation and algorithm development,” *IEEE Trans. Power Syst.*, vol. 30, no. 2, pp. 734–743, 2015.
- [61] R. Online *et al.*, “Online coordinated voltage control in distribution systems subjected to structural changes and DG availability Publication Details,” 2016.
- [62] P. C. Ramaswamy and G. Deconinck, “Relevance of voltage control, grid reconfiguration and adaptive protection in smart grids and genetic algorithm as an optimization tool in achieving their control objectives,” in *2011 International Conference on Networking, Sensing and Control, ICNSC 2011*, 2011, pp. 26–31.
- [63] S. Chakravorty, J. Chakravorty, and S. Sarkar, “Node voltage improvement by network reconfiguration: A soft computing approach,” in *ACT 2009 - International Conference on Advances in Computing, Control and Telecommunication Technologies*, 2009, pp. 687–691.
- [64] K. You and T. Reindl, “Voltage enhancement by basic active power curtailment of low-voltage grid-connected PV systems in view of complex power flow theories and real world testing and measurement results,” in *2017 Asian Conference on Energy, Power and Transportation Electrification, ACEPT 2017*, 2017, vol. 2017-Decem, pp. 1–8.
- [65] A. Latif, P. W. Gawlik, and P. P. Palensky, “A Controller for Fair and Coordinated Active Power Curtailment of Low Voltage PV Inverters,” no. Figure 1, pp. 1–13, 2015.
- [66] A. Singhal, V. Ajjarapu, J. Fuller, and J. Hansen, “Real-Time Local Volt/Var Control

- under External Disturbances with High PV Penetration,” *IEEE Trans. Smart Grid*, vol. 10, no. 4, pp. 3849–3859, 2019.
- [67] F. Ding and M. Baggu, “Coordinated Use of Smart Inverters with Legacy Voltage Regulating Devices in Distribution Systems with High Distributed PV Penetration — Increase CVR Energy Savings,” *IEEE Trans. Smart Grid*, vol. PP, no. c, p. 1, 2018.
- [68] A. Molina-Garcia, R. A. Mastromauro, T. Garcia-Sanchez, S. Pugliese, M. Liserre, and S. Stasi, “Reactive Power Flow Control for PV Inverters Voltage Support in LV Distribution Networks,” *IEEE Trans. Smart Grid*, vol. 8, no. 1, pp. 447–456, Jan. 2017.
- [69] M. Farivar, R. Neal, C. Clarke, and S. Low, “Optimal inverter VAR control in distribution systems with high PV penetration,” in *IEEE Power and Energy Society General Meeting*, 2012, pp. 1–7.
- [70] X. Su, M. A. S. Masoum, and P. J. Wolfs, “Optimal PV inverter reactive power control and real power curtailment to improve performance of unbalanced four-wire LV distribution networks,” *IEEE Trans. Sustain. Energy*, vol. 5, no. 3, pp. 967–977, 2014.
- [71] E. Dall’Anese, S. V. Dhople, and G. B. Giannakis, “Optimal Dispatch of Photovoltaic Inverters in Residential Distribution Systems,” *IEEE Trans. Sustain. Energy*, vol. 5, no. 2, pp. 487–497, Apr. 2013.
- [72] N. Yorino, T. Watakabe, Y. Nakamura, Y. Sasaki, Y. Zoka, and A. B. Khalifa Hussien, “A Novel Voltage Control Method for Distribution Systems based on P&Q Nodal Prices for Distributed Generations,” *IEEJ Trans. Power Energy*, vol. 139, no. 3, pp. 178–185, Mar. 2019.
- [73] S. N. Salih and P. Chen, “On coordinated control of OLTC and reactive power compensation for voltage regulation in distribution systems with wind power,” *IEEE Trans. Power Syst.*, vol. Accepted f, pp. 1–10, 2015.
- [74] A. Kulmala, S. Repo, and P. Jarventausta, “Coordinated voltage control in distribution networks including several distributed energy resources,” *IEEE Trans. Smart Grid*, vol. 5, no. 4, pp. 2010–2020, Jul. 2014.
- [75] K. M. Muttaqi, A. D. T. Le, M. Negnevitsky, and G. Ledwich, “A Coordinated Voltage Control Approach for Coordination of OLTC, Voltage Regulator, and DG to Regulate Voltage in a Distribution Feeder,” *IEEE Trans. Ind. Appl.*, vol. 51, no. 2, pp. 1239–1248, Mar. 2015.
- [76] L. Wang, F. Bai, R. Yan, and T. K. Saha, “Real-Time Coordinated Voltage Control of PV Inverters and Energy Storage for Weak Networks With High PV Penetration,” *IEEE Trans. Power Syst.*, vol. 33, no. 3, pp. 3383–3395, May 2018.
- [77] M. M. Othman, M. H. Ahmed, and M. M. A. Salama, “A Coordinated Real-Time Voltage Control Approach for Increasing the Penetration of Distributed Generation,” *IEEE Syst. J.*, pp. 1–9, Apr. 2019.
- [78] C.-H. Lin, H.-J. Chuang, C.-S. Chen, C.-S. Li, and C.-Y. Ho, “Fault Detection, Isolation and Restoration using a Multiagent-based Distribution Automation System.”
- [79] M. D’Inverno and M. Luck, *Understanding agent systems*. Berlin ; New York: Springer, 2001.
- [80] M. Schumacher, *Objective Coordination in Multi-Agent System Engineering: Design and Implementation*. Springer, 2001.
- [81] K. E. Antoniadou-Plytaria, I. N. Kouveliotis-Lysikatos, P. S. Georgilakis, and N. D. Hatzigaryriou, “Distributed and Decentralized Voltage Control of Smart Distribution Networks: Models, Methods, and Future Research,” *IEEE Trans. Smart Grid*, pp. 1–1, 2017.

-
- [82] Y. Wang, K. Tan, X. Peng, and P. So, "Coordinated Control of Distributed Energy Storage Systems for Voltage Regulation in Distribution Networks," *IEEE Trans. Power Deliv.*, vol. 8977, no. c, pp. 1–1, 2015.
- [83] A. G. Tsikalakis and N. D. Hatziargyriou, "Centralized Control for Optimizing Microgrids Operation," *IEEE Trans. ENERGY Convers.*, vol. 23, no. 1, 2008.
- [84] M. E. Elkhatab, R. El-Shatshat, and M. M. A. Salama, "Novel Coordinated Voltage Control for Smart Distribution Networks With DG," *Smart Grid, IEEE Trans.*, vol. 2, no. 4, pp. 598–605, 2011.
- [85] A. Bedawy and N. Yorino, "Reactive Power Control of DGs for Distribution Network Voltage Regulation Using Multi-Agent System," *IFAC-PapersOnLine*, vol. 51, no. 28, pp. 528–533, Jan. 2018.
- [86] A. Bedawy, N. Yorino, and K. Mahmoud, "Management of voltage regulators in unbalanced distribution networks using voltage/tap sensitivity analysis," in *2018 International Conference on Innovative Trends in Computer Engineering (ITCE)*, 2018, pp. 363–367.
- [87] "Distribution Test Feeders - Distribution Test Feeder Working Group - IEEE PES Distribution System Analysis Subcommittee." [Online]. Available: <https://ewh.ieee.org/soc/pes/dsacom/testfeeders/>. [Accessed: 10-Nov-2017].
- [88] "Grid-interconnection Code JEAC9701-2016."
- [89] K. P. Schneider *et al.*, "Analytic Considerations and Design Basis for the IEEE Distribution Test Feeders," *IEEE Trans. Power Syst.*, vol. 33, no. 3, pp. 3181–3188, May 2018.
- [90] "Resources | PES Test Feeder." [Online]. Available: <https://site.ieee.org/pes-testfeeders/resources/>. [Accessed: 19-Dec-2019].
- [91] M. E. Baran and F. F. Wu, "Network reconfiguration in distribution systems for loss reduction and load balancing," *IEEE Trans. Power Deliv.*, vol. 4, no. 2, pp. 1401–1407, 1989.
- [92] N. Yorino, M. Danyoshi, and M. Kitagawa, "Interaction among multiple controls in tap change under load transformers," *IEEE Trans. Power Syst.*, vol. 12, no. 1, pp. 430–436, 1997.

Appendix A: Description of Test Systems

Four distribution test feeders are employed for evaluating and testing the proposed methods in the thesis. The feeders include two unbalanced IEEE 34 and 123-node test feeders [89], [90], 33-bus distribution feeder, and five node test system. These systems have different configurations and structures and it can be described briefly as follows:

A.1 IEEE 34-node Test Feeder

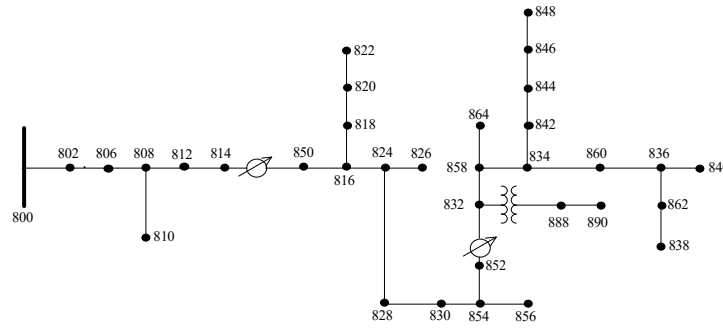


Figure A.1 IEEE 34-node test feeder

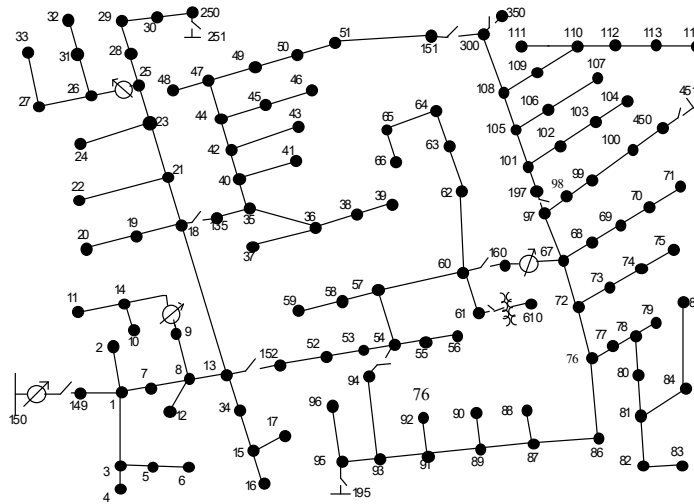


Figure A.2 IEEE 123-node test feeder

This feeder operates at a nominal voltage of 24.9 kV and it is characterized by long, lightly and unbalanced loading, two three-phase voltage regulators, shunt capacitors, 6 spot loads, and 19 distributed loads. The complete system data are given in [90]. The single line diagram of this system is shown in Figure A.1.

A.2 IEEE 123-node Test Feeder

The IEEE 123 node test feeder has a nominal voltage of 4.16 kV. This feeder is characterized by different configuration of overhead and underground lines, unbalanced loading, four voltage regulators, four shunt capacitor banks, and 11 switches. The complete system data are given in [90]. The single line diagram of this system is shown in Figure A.2.

A.3 33-Bus Distribution System

The 33-bus test system is a MV system with a single 12.66 kV supply point. The system consists of 33-buses, 3 laterals, and 32 branches. The total active and reactive loads powers are 3.715 MW and 2.3 Mvar, respectively. The complete system data are given in [91]. The single line diagram of this system is shown in Figure A.3.

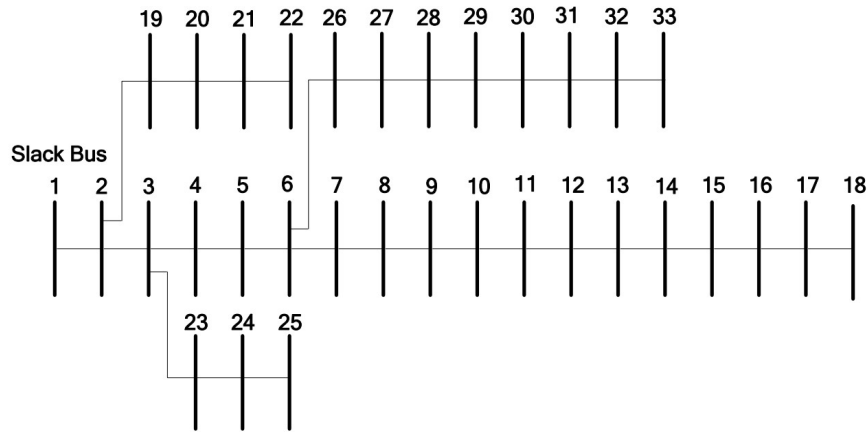


Figure A.3 33-bus test feeder

A.4 5-bus Test Feeder

A test feeder consists of 5-bus and four PV sources as shown in Figure A.4 is used to check the performance of the voltage control method using nodal prices which described in Chapter 5. The 5-bus feeder operates at nominal voltage 6.6-kV and it has the following data.

Base power $P_B = 3$ [MVA], Base voltage

$V_B = 6.6$ [kV].

Line impedance $Z_i = 0.04 + j0.04$ [p. u.].

Customer load $S_{li} = 0.02$ [p. u.].

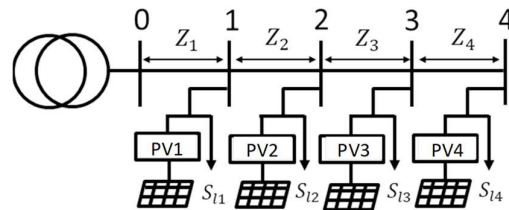


Figure A.4 5-bus test feeder

Appendix B: The Optimality of the Voltage Regulators Control Strategy

This appendix explains the optimality of the proposed control method discussed in Chapter 3 for the voltage regulators from the mathematical viewpoint based on [92]. The equivalent forms to objective functions (3.1) and (3.2) are as follows:

$$\min U(t) = \sum_{t=0}^{\infty} VD_{abc}(\mathbf{u}(t)) \quad (\text{B.1})$$

$$VD_{abc}(\mathbf{u}(t)) = \frac{1}{2} \sum_{k=1}^N w_k (\mathbf{u}_k(t))^2 \quad (\text{B.2})$$

In this equation, $\mathbf{u}(t)$ is the voltage deviation vector at time t and defined as

$$\mathbf{u}(t) = \mathbf{g}(\mathbf{v}(t)) = \mathbf{vc}(t) - \mathbf{vc}_R \quad (\text{B.3})$$

where, $\mathbf{u}(t) = [u_1(t), u_2(t), \dots, u_N(t)]^T$,

$\mathbf{vc} = [vc_1, vc_2, \dots, vc_N]$ vector of center voltages defined in (20).

$\mathbf{vc}_R = [vc_{R1}, vc_{R2}, \dots, vc_{RN}]$ vector of target center voltages.

Equation (B.2) becomes minimal in the neighborhood of $\mathbf{u} = \mathbf{0}$, which is referred to as the equilibrium area in this research and expressed as follows:

$$E = \{u_1, u_2, \dots, u_N \mid |u_k| < \varepsilon_k, k = 1, \dots, N\} \quad (\text{B.4})$$

with ε_k : dead band of tap k .

Then, we set another objective defined as

$$\min T, \mathbf{u}(T) \in E \quad (\text{B.5})$$

T : number of tap operations to reach the equilibrium from $t=0$.

The voltages in UDS are governed by the power flow equations, and they are the function of tap positions of voltage regulators n and load parameters L , as described in (3.3).

$$\mathbf{v} = \mathbf{f}(\mathbf{L}, \mathbf{n}) \quad (\text{3.3})$$

The linearization of (3.3) with $\mathbf{v}(t)$ at time t around the target voltage with tap control $\mathbf{Z}(\mathbf{v}(t))$ and load disturbance $\Delta \mathbf{L}(t)$ yields

$$\mathbf{u}(t+1) = \mathbf{u}(t) + \tilde{\mathbf{A}}(t) \cdot \mathbf{Z}(t) + \mathbf{B}(t) \cdot \Delta \mathbf{L}(t) \quad (\text{B.6})$$

where

$$\tilde{\mathbf{A}}(t) = \mathbf{A}(t) \cdot \mathbf{R}, \quad \mathbf{A}(t) = [a_{ij}] = \left[\frac{\partial g}{\partial v} \cdot \frac{\partial v}{\partial n} \right]_{\substack{n=n(t) \\ L=L(t)}} \in \mathbb{R}^{N \times N},$$

$$\mathbf{B}(t) = [\partial v / \partial L]_{\substack{n=n(t) \\ L=L(t)}} \in \mathbb{R}^{N \times P}, \quad \Delta \mathbf{L}(t) = \mathbf{L}(t+1) - \mathbf{L}(t),$$

$$\mathbf{Z}(t) = \mathbf{R}^{-1} \Delta n(t) = \mathbf{R}^{-1} (n(t+1) - n(t)) = [Z_1(t), Z_2(t), \dots, Z_N(t)]^T$$

$\mathbf{R} = \text{diag} [r_1, r_2, \dots, r_N]$: regulator step size.

Equation (B.2) represents a dynamic system with disturbance $\Delta \mathbf{L}(t)$ and control $\mathbf{Z}(t)$.

Then, we find the optimal control $\mathbf{Z}(t)$ under the following assumptions.

- a) At each time t , only one tap can act, i.e., only one component of $\mathbf{Z}(t) = [Z_1(t), Z_2(t), \dots, Z_N(t)]$ is “+1” or “-1”, and the others are “0” (see (3.5)).
- b) Linearization errors are neglected in the control problem (B.1) -(B.6).
- c) The initial voltage deviation $\mathbf{u}(0)$ is \mathbf{u}^0 ($\mathbf{u}(0) = \mathbf{u}^0$).
- d) Future load disturbances are unknown, which are treated as $\Delta \mathbf{L}(\tau) = 0$, $\tau = t, t+1, \dots$.

Minimization of the voltage deviations (A1)

The change in (B.2) at time t is described as follows:

$$\Delta VD_{abc}(\mathbf{u}(t)) = VD_{abc}(\mathbf{u}(t+1)) - VD_{abc}(\mathbf{u}(t)) \quad (\text{B.7})$$

If the control is executed to satisfy $\Delta VD_{abc}(t) < 0$, VD_{abc} satisfies the condition of Lyapunov function for the dynamic system. According to the Lyapunov stability criterion, the asymptotic stability of the system (B.6) is guaranteed. Therefore, if there is an equilibrium point, the system converges to the equilibrium area E within the finite step T .

$$u(t) = u^e \in E, \quad t \geq T \quad (\text{B.8})$$

If there is no equilibrium point, the system converges to a certain point that minimizes VD_{abc} .

Now, Lyapunov function at time T , (B.2), is expressed as follows:

$$VD_{abc}(T) = \sum_{\tau=0}^{T-1} \Delta VD_{abc}(\tau) + VD_{abc}(0) = 0 \quad (\text{B.9})$$

Assuming that $u^e \approx 0$ due to (A8) at $t=T$,

$$\begin{aligned}
 U &= \sum_{t=0}^T VD_{abc}(t) \\
 &= (T+1) \cdot VD_{abc}(0) + T \cdot \Delta VD_{abc}(0) + (T-1) \cdot \Delta VD_{abc}(1) + \\
 &\quad \dots + \Delta VD_{abc}(T-1) \\
 &= (T+1) \cdot VD_{abc}(0) + \sum_{t=0}^{T-1} (T-t) \cdot \Delta VD_{abc}(t)
 \end{aligned} \tag{B.10}$$

In (B.10), the first term of the right-hand side is constant, and the others are the sum of positively weighted (1, 2, ..., T) terms. Minimizing each term by the descending order of weight coefficients (T+1, T...) will minimize the overall VD_{abc} . The condition to minimize U is as follows:

$$\Delta VD_{abc}(0) < \Delta VD_{abc}(1) < \Delta VD_{abc}(T-1) < 0 \tag{B.11}$$

This condition is equivalent to the following minimization at each time t :

$$\min \Delta VD_{abc}(t) \quad t = 0, 1, 2, \dots \tag{B.12}$$

Minimization of tap operations (A5)

Assuming the initial tap position $\mathbf{n}(0) = \mathbf{n}^0$ and equilibrium point position $\mathbf{n}(T) = \mathbf{n}^e$, the number of tap changes required to the equilibrium point is

$$\mathbf{K}^e = R^{-1}(\mathbf{n}^0 - \mathbf{n}^e) \tag{B.13}$$

In this equation, \mathbf{K}^e is a vector whose components are integers K_i^e . In other words, K_i^e corresponds to the minimum number of necessary tap changes of each tap i to reach the equilibrium point. Therefore, the minimum of tap changes T is given by

$$T \geq \|\mathbf{K}^e\|_1 = \sum_{i=1}^N |K_i^e| \tag{B.14}$$

The minimum step $\|\mathbf{K}^e\|_1$ can be determined if \mathbf{n}^0 and \mathbf{n}^e are given. To reach the equilibrium within the above minimum steps, the norm of (B.15) must be reduced by one step at each time t to satisfy (B.16).

$$\mathbf{K}(t) = R^{-1}(\mathbf{n}(t) - \mathbf{n}^e) \tag{B.15}$$

$$\|\Delta \mathbf{K}(t)\|_1 = \|\mathbf{K}(t+1)\|_1 - \|\mathbf{K}(t)\|_1 \leq -1 < 0 \tag{B.16}$$

Equation (B.16) implies that $\mathbf{n}(t)$ reaches \mathbf{n}^e with the minimum step if it is controlled step by step toward \mathbf{n}^e . Therefore, the control to minimize (B.1) also satisfies (B.16) and (B.5). Note that the conditions for oscillatory action have been analyzed in [92], where (B.5) and (B.16) are violated.

Control rules

Now, substituting (B.6) into (B.1), we obtain

$$\begin{aligned}
 \Delta VD_{abc}(\mathbf{u}(t)) &= VD_{abc}(\mathbf{u}(t+1)) - VD_{abc}(\mathbf{u}(t)) \\
 &= \mathbf{S}_{abc}(\mathbf{u}(t)) \cdot \mathbf{Z}(t) + \mathbf{Z}(t)^T \cdot \mathbf{C} \cdot \mathbf{Z}(t) \\
 &= \sum_i (S_{abci}(u) \cdot Z_i + Z \cdot |C_{ii}| \cdot |Z_i|) \\
 &\approx \sum_i S_{abci}(u) \cdot Z_i
 \end{aligned} \tag{B.17}$$

where

$$\begin{aligned}
 \mathbf{S}_{abc}(\mathbf{u}(t)) &= \mathbf{u}(t)^T \cdot \mathbf{M} \cdot \tilde{\mathbf{A}}(t), \\
 \mathbf{C} &= \tilde{\mathbf{A}}(t)^T \cdot \mathbf{M} \cdot \tilde{\mathbf{A}}(t)
 \end{aligned} \tag{B.18}$$

In this equation, since $C_{ii} \approx 0$ has been numerically confirmed, (B.17) holds. Then, the optimal control rule of (3.9) is obtained. Thus, (B.12) is minimized as follows:

➤ **Optimal Control Rule**

When there is voltage violation at time t , a controller that minimizes $\Delta VD_{abc}(t)$ is selected. In other words, at each time t , we select at most one controller k that satisfies (B.19).

$$s_k(u) = \max_i |s_i(u)| > \alpha \tag{B.19}$$

with α : threshold value.

This control rule provides the order of controller actions to minimize the objective function.

➤ **Suboptimal Control Rule**

A simple autonomous control rule is given as follows:

At each time t , the controller that satisfies (B.20) is activated.

$$\begin{aligned}
 u_k(t) &> \varepsilon_k \text{ AND } s_k(u_e(t)) > \alpha_0 \text{ [Up]} \\
 u_k(t) &< -\varepsilon_k \text{ AND } s_k(u_e(t)) < -\alpha_0 \text{ [Down]}
 \end{aligned} \tag{B.20}$$

According to this rule, each controller can act independently based on its own index S and threshold value α_0 . The suboptimal control does not provide strict optimality, since in rare cases, it simultaneously allows multiple controls, which may change the optimal sequence of controls given by (B.19).

Appendix C: Conventional Method for PV Inverter Control

The conventional method is a typical local control scheme used in the Japanese system for the PV inverter [88]. The PV power generation is maximum ($P=P_{\max}$, $Q=0$) when the voltage is within limits. When the voltage hits the limit, the PV inverter acts as shown in Figure C.1, which is explained as follows:

- [Step 1] Increase reactive power output and reduce active power generation to regulate the voltage within limits.
- [Step 2] When the PV inverter operating point reaches the power factor limit (0.85), fix the power factor and reduce the power output for the voltage control.

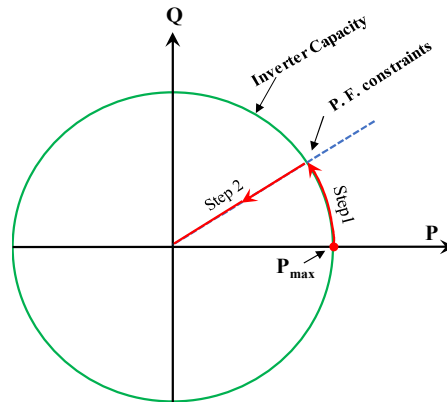
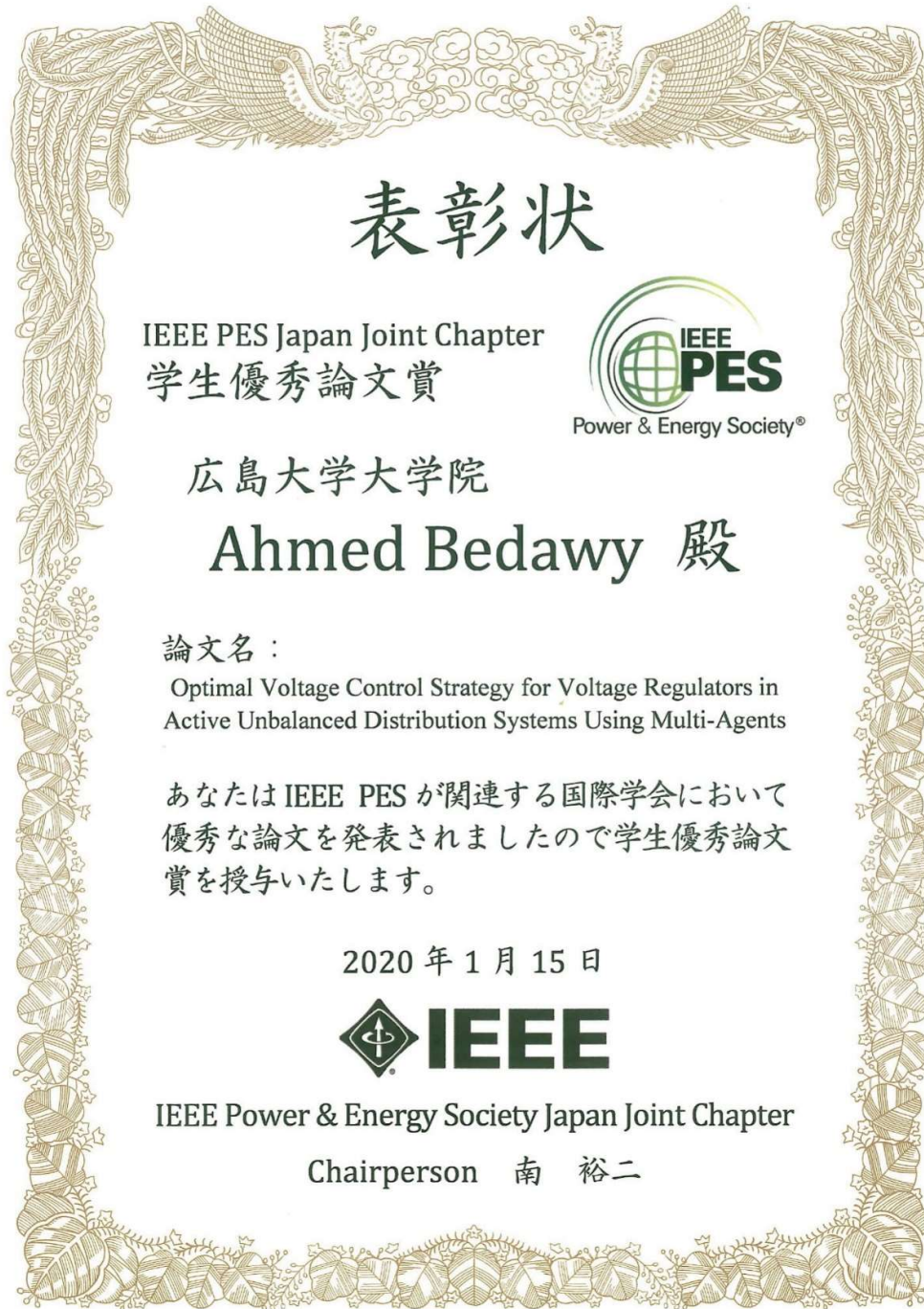


Figure C.1 Inverter control scheme for conventional method.

Appendix D: IEEE PES Japan Joint Chapter Best Paper Award



List of Publications

A. Transactions/ International Journal Papers

- A-(1) **A. Bedawy**, N. Yorino, K. Mahmoud, Y. Zoka, and Y. Sasaki, 'Optimal Voltage Control Strategy for Voltage Regulators in Active Unbalanced Distribution Systems Using Multi-Agents', *IEEE Transactions on Power Systems*, vol. 35, no. 2, pp. 1023-1035, March 2020.
- A-(2) N. Yorino, T. Watakabe, Y. Nakamura, Y. Sasaki, Y. Zoka, and **A. Bedawy**, "A Novel Voltage Control Method for Distribution Systems based on P&Q Nodal Prices for Distributed Generations," *IEEE Trans. Power Energy*, vol. 139, no. 3, pp. 178–185, Mar. 2019.
- A-(3) Y. Zoka, S. Hosoda, M. Watanabe, T. Kurushima, **A. Bedawy**, Adelhard B. Rehiara, Y. Sasaki, N. Yorino, 'An effective method for distributed voltage control on system reconfiguration and improper motion of voltage control devices for distribution networks', *IEEE Trans. Power Energy*, vol. 138, no. 1, pp. 14–22, 2018.

B. International Conference Papers Related to This Thesis

- B-(1) **A. Bedawy** and N. Yorino, 'Reactive Power Control of DGs for Distribution Network Voltage Regulation Using Multi-Agent System', *IFAC-PapersOnLine*, vol. 51, no. 28, pp. 528–533, Sep. 2018.
- B-(2) **A. Bedawy**, N. Yorino and K. Mahmoud, "Management of voltage regulators in unbalanced distribution networks using voltage/tap sensitivity analysis," *2018 International Conference on Innovative Trends in Computer Engineering (ITCE)*, Aswan, 2018, pp. 363-367.
- B-(3) **A. Bedawy**, N. Yorino and K. Mahmoud, "Optimal decentralized voltage control in unbalanced distribution networks with high PV penetration," *2017 Nineteenth International Middle East Power Systems Conference (MEPCON)*, Cairo, 2017, pp. 1373-1377.

Contents of the Thesis and Published Papers Relationship

Chapters	Title of chapters	Published papers
Chapter 1	Introduction	A-(1), A-(2), A-(3), B-(1), B-(2), B-(3)
Chapter 2	Voltage Control in Distribution Systems	A-(1), A-(2), A-(3), B-(1), B-(2), B-(3)
Chapter 3	Optimal Voltage Control Strategy for Voltage Regulators in Active UDS	A-(1), A-(3), B-(2), B-(3)
Chapter 4	Reactive Power Control of DGs for Voltage Regulation	B-(1)
Chapter 5	Active/Reactive Power Control of DGs Using Nodal Prices	A-(2)
Chapter 6	Conclusions and Future works	A-(1), A-(2), A-(3), B-(1), B-(2), B-(3)